HHS Public Access

Author manuscript

Compr Physiol. Author manuscript; available in PMC 2016 October 01.

Published in final edited form as:

Compr Physiol. ; 5(4): 1623–1644. doi:10.1002/cphy.c140070.

Biomechanics of Cardiac Function

Andrew P. Voorhees and **Hai-Chao Han***

Department of Mechanical Engineering, The University of Texas at San Antonio, Biomedical Engineering Program, UTSA-UTHSCSA

Abstract

The heart pumps blood to maintain circulation and ensure the delivery of oxygenated blood to all the organs of the body. Mechanics play a critical role in governing and regulating heart function under both normal and pathological conditions. Biological processes and mechanical stress are coupled together in regulating myocyte function and extracellular matrix structure thus controlling heart function. Here we offer a brief introduction to the biomechanics of left ventricular function and then summarize recent progress in the study of the effects of mechanical stress on ventricular wall remodeling and cardiac function as well as the effects of wall mechanical properties on cardiac function in normal and dysfunctional hearts. Various mechanical models to determine wall stress and cardiac function in normal and diseased hearts with both systolic and diastolic dysfunction are discussed. The results of these studies have enhanced our understanding of the biomechanical mechanism in the development and remodeling of normal and dysfunctional hearts. Biomechanics provide a tool to understand the mechanism of left ventricular remodeling in diastolic and systolic dysfunction and guidance in designing and developing new treatments.

Introduction

The heart pumps blood and nutrients to all organs to support their normal function. Synchronized contraction of the myocardium generates pressure to drive the blood flow in arteries to distal organs and the constant repetitive pumping action maintains the circulation to all organs. Biomechanical principles play an important role in governing cardiac function.

Many diseases may affect the complex pumping system of the heart, and can be caused by a variety of factors including genetic defects, aging, and environmental stimuli. Left ventricular (LV) myocardial infarction (MI) due to coronary heart disease and diastolic dysfunction due to hypertension and LV hypertrophy are two major forms of heart disease. Biomechanics plays a critical role in regulating cardiac function not only in the normal heart but also in the diseased heart. Knowledge of the biomechanics of the heart is requisite for understanding the causes and consequences of cardiac diseases. For example, mechanical stress plays an important role in the development of cardiomyopathy and LV remodeling post-MI, regulating tissue fibrosis and scar formation. Altering the mechanical stress patterns can provide effective approaches for treatment of MI and improving cardiac function. Increased stresses in the myocardium due to hypertension can also lead to

*Corresponding author, hchan@utsa.edu.

hypertrophy of the ventricles and diastolic heart failure. While heart valve diseases, either stenosis or insufficiency (regurgitation) also have a direct effect on the pumping function of the heart, we intend to primarily focus our discussion on the myocardial wall and LV function. We will provide a brief discussion of the biomechanical studies of the right ventricle, atria and heart valves and refer readers to recent reviews in the fields.

This paper reviews the relevant biomechanical concepts and measurements and summarizes the recent advances in the biomechanics of LV in MI and diastolic dysfunction as well as related treatments. It is concluded that biomechanical knowledge and research are required to fully understand the causes of cardiac dysfunction and develop new treatment devices and techniques.

Biomechanics of Normal Cardiac Function

The heart is a multiscale system that functions at the organ, tissue, cellular, and protein levels. Cardiac function can be evaluated at the cellular, tissue and organ levels, and at each level mechanical stress plays an important role in regulating function. This section will examine the measurement of cardiac function and the role of mechanics in determining cardiac function at each of these length scales in the healthy heart.

Cardiac Function

The primary function of the LV is to pump blood to distal organs and all the extremities of the body. The performance of the pump depends on the contraction force of the myocardium, the loading conditions, ventricular size and shape, and valve function. Heart failure occurs when the LV is unable to meet the demands of the body. Biomechanics is a major determinant of cardiac function. Therefore, it is important to be able to describe and measure cardiac function.

The Ventricular Pressure Volume Relationship—The cardiac cycle, a single beat of the heart, is typically divided into two phases: systole, the period of active contraction, and diastole the period of relaxation and filling. At the onset of the systolic phase the LV of the heart is filled with blood to a pressure of about 8 mm Hg and a pressure of greater than 16 mm Hg being considered abnormal (152, 154). At this point both the mitral valve that leads into the LV and the aortic valve through which blood leaves the chamber are closed. Active contraction of the myocytes in the myocardium of the LV rapidly raises the fluid pressure above the pressure in the aorta. This period of systole is referred to as isovolumic contraction since blood is not flowing into or out of the LV. Once the fluid pressure inside the LV surpasses the pressure in the aorta, the aortic valve opens and the contraction of the myocardium pushes the pressurized blood out of the chamber and into circulation. This phase is known as ejection. As the contractile force generated by the myocytes diminishes the pressure of the blood in the LV chamber again falls below the systemic circulatory pressure and the aortic valve closes marking the end of the ejection phase and the end of systole. Relaxation of the myocytes causes a rapid isovolumic pressure drop in the blood remaining in the LV chamber, during the first phase of diastole known as isovolumic relaxation. When the pressure of the blood in the LV falls below the pressure of the left atria, the mitral valve opens causing the LV chamber to fill with blood. Finally the contraction of

the atria forces in the last bit of blood and slightly pressurizes the chamber to its end-diastolic pressure. This phase of the cardiac cycle is referred to as the filling or diastolic filling phase.

The overall performance of the pump depends on the contraction force of the myocardium, the loading conditions, ventricular size and shape, and valve function among others (Table 1).

In terms of mechanics, the best way to depict the cardiac cycle is using a pressure-volume diagram (Figure 1.A). The PV diagram depicts the cardiac cycle as a counterclockwise loop. The right and left halves of the loop correspond to the isovolumic contraction and isovolumic relaxation phases while the bottom segment represents the filling phase and the top segment represents the ejection phase. The area contained within the loop is referred to as the stroke work (SW) and represents the amount of energy imparted by the LV into the blood. SW is a measure of how hard the heart is working. Despite being a relatively simple measure SW is often miscalculated in the literature and reported with incorrect units (170). Sarnoff and Berglund were the first to report SW, and they calculated SW as gram-force-meters, but listed the units simply as gram-meters (169). The distinction between grams and grams-force is subtle and has led to much misreporting. The correct units for SW should be units of work such as Joules, or simply mm Hg-ml. The heart is capable of adjusting the amount of work it does in order to match the metabolic demands of the body.

Plotting different cardiac cycles with varied end-diastolic volumes on one plot allows for two important mechanical relationships to be determined, the end-diastolic pressure volume relationship (EDPVR) and the end-systolic pressure volume relationship (ESPVR) (Figure 1.B). The EDPVR can be measured by varying the amount of diastolic filling through temporarily occluding of the vena cava, a common technique in animal studies (12, 31). The EDPVR represents the relationship between the diastolic pressure and the diastolic volume. Increasing the diastolic volume stretches the myocardial tissue which puts stress on the tissue and increases the pressure of the blood. In this way the curve is a representation of the passive mechanical properties of the myocardial tissue with volume being equivalent to strain and pressure being equivalent to the stress. Diastolic pressure volume curves are typically exponential matching the exponential stress-strain behavior of most biological soft tissues. One of the foundational principles of ventricular mechanics is the Frank-Starling mechanism, also called Starling’s Law of the Heart. This principle states that increasing diastolic filling will increase the stroke volume of the heart (151). This can be seen by looking at the PV curves and seeing that as the volume of blood during diastole increases, the end-diastolic point on the EDPVR moves further away from the ESPVR which increases the stroke volume. From a physiological standpoint this occurs due to the fact that the added diastolic filling stretches the sarcomeres of the myocytes which in turn allows them to generate more force per contraction (71). Diastolic dysfunction can occur when the ventricle becomes too stiff resulting in a leftward and upward shift of the EDPVR and adverse remodeling can lead to dilation of the ventricle which leads to a right shift in the EDPVR (Figure 1.C) (131).

The end-systolic pressure volume relationship represents the amount of blood left in the ventricle for a given aortic blood pressure. The higher the aortic blood pressure, the less blood that is able to leave the LV. The ESPVR is typically a linear relationship and the slope of the ESPVR is called the maximum elastance (168). The maximal elastance is considered a measure of the contractile ability of the LV for a given inotropic state. Changes in the inotropic state which could be due to the influence of signaling hormones such as epinephrine or drugs such as beta blockers alter the maximal elastance which can raise or lower the amount of blood the LV is able to eject (30). Inotropic agents are currently under investigation as potential therapies for heart failure, but trials have been met with mixed success (137).

Stroke Volume and Ejection Fraction—There are many different parameters that are used to quantify the function of the heart (Table 2). However, since the primary function of the heart is to pump blood through the body, the most useful measures quantify the actual volume of blood being pumped. Stroke volume (SV) is defined as the difference between the LV volume at end-diastole (EDV) and end-systole (ESV), or in other words the width of the pressure-volume loop.

$$SV = EDV - ESV \quad (1)$$

While SV represents how much blood the heart pumps per beat, another parameter, ejection fraction (EF) is often used to describe heart function. EF is defined as

$$EF = \frac{SV}{EDV} \times 100 \quad (2)$$

EF is normalized by the end-diastolic volume so as to normalize the amount of blood to the actual size of the LV, which accounts for differences in size between patients. In humans, ejection fraction is typically between 50 and 80% and readings below this level are a sign of heart failure (35).

Cardiac output is defined as the volume of blood a heart pumps per minute.

$$CO = SV \times HR \quad (3)$$

Where *HR* is the heart rate. CO is an important index of overall heart function. CO increases as body demand goes up such as in physical exercise. CO depends on many factors and myocardial contractility is only one of these factors.

Measuring Cardiac Function

There are many options for measuring cardiac function including both invasive and noninvasive methods (Table 3). Clinically, the first choice in measurement techniques is often echocardiography as it is relatively inexpensive, portable and does not rely on ionizing radiation (43). Echocardiography allows for coarse evaluation of cardiac dimensions

throughout the cardiac cycle. This allows for the calculation of LV volumes and wall thicknesses. Improvements in echocardiography over the last decade now allow for three dimensional imaging, which can improve the estimate of LV chamber volumes (93). The speed and portability of echocardiography make it well suited to the research lab as well. CT scans are also commonly employed to measure cardiac function, and they may give added resolution as compared to echocardiography. However, they come with added expense and radiation dose to the patient and may not be the first choice for examining LV function. MRIs can offer very detailed geometries of the LV, but due to imaging times, as well as costs may not be the best choice. A Multi Gated Acquisition Scan (MUGA) is another clinical option for measuring cardiac volumes. During this test a radioactive tracer is injected into the blood stream and the LV is imaged with a gamma camera that detects the gamma particles emitted by the tracer. This method is highly accurate but is typically reserved for patients who have already been diagnosed with heart disease. CT, MRI and MUGA all require the use of a gating system which utilizes the patient's ECG signal to reconstruct accurate LV volumes at various points throughout the cardiac cycle based on several successive cardiac cycles.

While, volumetric measurements are a good measure of the overall ventricle function, they do not capture the whole biomechanical picture. Measurement of local myocardial contraction and wall strain has been used as another important index of cardiac function. Early studies relied on the implantation of radiopaque markers on to the surfaces of the LV which allowed for their motion to be tracked by radiographic methods (4, 42, 197) Advances in MRI technology now allow for virtual tags to be placed on the heart and their motion tracked throughout the cardiac cycle in order to examine local tissue deformation (140, 224). Tags can be placed by creating small tissue regions with distinct magnetic properties, which can be achieved through magnetic saturation of these regions or spatial variations in the magnetic field gradient (89). For a review of strain analysis techniques using MRI please see the 2014 article by Jiang, et al (89). Another recent advance is the development of speckle-tracking echocardiography and Doppler tissue imaging which both allow for the calculation of regional tissue strains (1, 66, 186). The use of ultrasonic contrast agents such as microspheres can aid in the measurement of local tissue deformation by more clearly defining the boundary between blood and tissue (129). A nice overview of echocardiograpic strain analysis techniques can be found in the review by Gorcsan et al (56). Local strains of the LV wall during the cardiac cycle give a direct measurement of tissue contractile ability and can identify regions of tissue that are not contracting properly. The global or averaged longitudinal strain has become a widely used clinical measurement (93, 185). In a healthy population longitudinal strain was found to have 95% confidence intervals of −17.0-28.9% while the confidence interval for radial strain was found to be 40.1-82.0% (101). Values that are nearer to 0 are a strong indicator of heart failure (141).

Echocardiographic strain analysis has also allowed for the calculation of strain rates which can provide insight into dynamics of contraction. Speckle tracking echocardiography has also become an important tool in the quantification of LV twist. Twist of the LV is an important component of cardiac function and reduction in LV twist has been associated with several forms of cardiac disease (141). In a cohort of healthy humans, peak LV systolic twist was found to be 6.7 degrees in young patients, 8.0 degrees in middle aged patients, and 10.8

degrees in older patients (183). The rate and amount of untwisting during diastole is also an important measure of diastolic function (4, 23, 183).

Doppler imaging technologies have also allowed for the calculation of mitral inflow velocities as well as the annular velocities of the mitral valve. The variable E is used to represent the peak mitral inflow velocity or peak E wave velocity. The variable e' is used to denote the annular velocity of the mitral valve during the early, E wave period of diastole. These values are an important measure of diastolic function and the ratio of the mitral inflow velocity to the early diastolic annular velocity (E/e') is an excellent predictor of the end-diastolic LV pressure (144).

Cardiac catheterization is an invasive technique in which a catheter containing a pressure sensor, or now commonly a pressure and volume sensor is inserted into the heart through the aorta. Guidance of the catheter is often aided by the use of a fluoroscope which can be used to determine the position of the catheter in the heart. This technique can be used to determine the pressure volume loops and can be used to determine if there are any unusual pressure gradients in the LV which could indicate areas of dysfunction (64). Two common measurements determined by cardiac catherization include the dP/dt which is the rate at which the pressure increases during systole and τ which is the time constant of ventricular relaxation. dP/dt is used in diagnosing systolic dysfunction while abnormally high values of τ denote diastolic dysfunction and can be an indicator of hypertrophy (19).

Cardiac catheterization is commonly employed in the research lab. One important test of mechanical function conducted with the use of pressure volume catheters is the occlusion test. During the measurement process, the inferior vena cava is temporarily occluded using a suture. This reduces the amount of filling in the LV which through the Frank-Starling mechanism reduces the amount of contractile force. By recording the PV loops for several different end-diastolic volumes, both the EDPVR and the ESPVR can be measured.

These measurements provide input for further mechanical analysis of cardiac function. Clinically, it provides references for the diagnosis of heart diseases.

Mechanical Properties of the Myocardium

In order to properly discuss the mechanics of the heart, it is necessary to clarify some of the mechanical engineering terms used in this review. Broadly, mechanics refers to the relationship between the forces applied to an object (solid or fluid) and the translation, rotation, and deformation generated as a result of the applied force. Mechanical stress (σ) describes the intensity of the mechanical force (loads) and mechanical strain describes the intensity of the deformation (elongation and angular rotation of a line in an object), thus stress has a unit of force per area while the strain is non-dimensional. Stretch or stretch ratio (λ) is a simple measure of deformation that is defined as the deformed length of a line segment divided by its initial undeformed length. For cardiovascular tissues that undergo large deformations, there are several different methods to define the stress and strain based on the reference configuration chosen. In cardiovascular mechanics, stress is most commonly reported as the Cauchy stress (or true stress) which is defined as the force over a unit area acting in the deformed configuration. Since, real-world mechanical problems are

three dimensional, stress and strain are represented as tensors, with nine components. Traditionally, cardiovascular solid mechanics has employed the framework of continuum mechanics, which assumes that the object (solid or fluid) has a continuous distribution of mass, meaning that there are no spaces or gaps in the material. This obviously does not capture the fact that materials are made of atoms and molecules and the use of continuum mechanics in biology is typically limited to the tissue level and larger. The phrase, "mechanical properties" as used in this review refers to the innate relationship between stress and strain of the tissue that governs how that tissue deforms under load. The mechanical properties of a tissue are described by the strain energy density (W) which describes how the mechanical energy in the tissue changes as a result of the deformation of the tissue. Thus it can be used as a measure of how much force or stress is needed to deform the tissue. The equations used to model the strain energy density are termed constitutive equations. The mechanical properties are determined by the structure and organization of the myocardial wall, the properties of both the intracellular and extracellular structural proteins, and the local mechanical stresses.

Ventricular Wall Structure—The ventricular wall is well known for its complex structure. The myofibers wrap around in layered sheets with rotating orientation. Across the wall thickness in the mid-ventricle, from endocardium to epicardium, the fiber direction changes from longitudinal to circumferential and then towards the longitudinal direction again.

Myocytes occur in sheets that are parallel to the epicardial surface of the heart. The myocytes in the sheet nearest to the epicardial surface of the heart tend to align at a negative angle with respect to the circumferential axis, while myocytes in the sheet nearest the endocardial surface tend to align in a direction with a positive angle with respect to circumferential axis. The exact amount of rotation has been shown to vary depending on the exact location within the LV (75). Furthermore, the orientation and amount of rotation of the myocytes varies depending on the location within the heart (60). The heterogeneity of myocyte orientation and the rotation of the myocytes through the thickness of the myocardium has many interesting mechanical implications. First of all it provides the tissue with strength in both the longitudinal and circumferential directions, the two directions that will experience the highest stresses. Secondly, it leads to the generation of ventricular torsion when the myocytes contract and relax (4). This arises because the inner surface of the myocardium is contracting in a different direction than the outer surface. Ventricular torsion is also partially due to differences in the timing of the electrical contraction signal between the subepicardial and subendocardial layers of the LV (22).

Cellular and Extracellular Determinants of Mechanics—The mechanical properties of the left ventricle are determined by both the properties of the cells, primarily the myocytes, and the extracellular matrix. In healthy myocardial tissue the passive mechanical properties are primarily determined by the intracellular protein titin. Titin is a large elastic protein that connects the z-line of the sarcomere to the m-line (Figure 2). The stiffness of the titin molecule prevents overextension of the sarcomere preventing damage to the cells. Given the abundance of myocytes in the myocardial tissue, titin is considered to be the primary

determinant of the passive mechanical properties of the healthy LV under low to moderate deformations (76). Interestingly, titin has many isoforms with some variants being significantly less stiff than others, and differences in the expression of these isoforms could play a role the development of diastolic dysfunction and heart failure (208). Further mutations of the titin gene have been associated with a number of various cardiomyopathies (117). Titin also plays an important role in cellular mechanotransduction as well as force generation (116). Phosphorylation of titin has been shown to be a means of altering the passive stiffness of the protein (80).

Since titin is a fibrous protein, it primarily provides stiffness in the fiber direction (along the length of the sarcomere). This makes myocardial tissue an anisotropic material. However, the myocytes of the heart do not align all in the same direction.

While titin determines the passive mechanical properties of the tissue, the active contractile force is generated by the interaction of the actin and myosin filaments. Myosin is a motor protein consisting of a head domain and a tail domain. The head domain is capable of binding to the actin protein that runs parallel to the myosin along the length of the sarcomere. Powered by the hydrolysis of adenosine triphosphate (ATP), the myosin head undergoes a conformational change that generates tension on the actin fiber. Following this conformational change, the myosin detaches from the actin filament, binds new ATP and then reattaches to the actin filament in a new location. This cyclic process allows for the myosin heads to essentially “walk” down the actin filaments resulting in the contraction of the sarcomere. The stiffness of the myocardial wall during active contraction is largely dictated by the number of myosin actin crossbridges that are engaged (32). The amount of force that can be generated by the sarcomere depends upon three key factors:1. The concentration of calcium ions released in response to the action potential, which activates the myofilaments to trigger contraction, 2. The phosphorylation state of the myosin chains which alters the stiffness of the myosin, 3. The length of the sarcomere which depends on both the preload and afterload placed on the ventricle (132). Both myosin and actin proteins have different isoforms, and changes in the relative amounts of the isoforms can lower contractility and are associated with the development of heart failure (219). Mutations in the genes for myosin are associated with both inherited dilated cardiomyopathy and hypertrophic cardiomyopathy (134). The coupling between the electrical signaling system and the mechanics of the heart is highly complex and was recently discussed in detail by Pfeiffer et al (156).

The extracellular matrix of the myocardium is composed of structural proteins such as collagen and elastin as well as non-structural proteins such as proteoglycans, proteases, and growth factors. From a mechanical standpoint, the most important of these proteins is collagen, which is primarily found as collagen I and collagen III, however collagen I is much stiffer than collagen III and as such is the primary controller of myocardial tissue properties under large deformation (205). Other collagen types, such as collagen IV, V, and VI are present in the ECM as well and although, they don’t directly contribute much to the mechanical properties of the tissue they have been shown to play important roles in collagen fiber formation and cell-matrix interactions (174). Fibronectin is another important ECM protein involved in regulating and facilitating the assembly of collagen I, however

fibronectin, on its own, is not a primary determinant of tissue mechanical properties. Fibronectin is an important mediator of LV remodeling (92, 175). Collagen I is a relatively stiff protein with a highly non-linear stress strain profile. Collagen provides little resistance at low amounts of stretch but large amounts of resistance at large stretches (48). Collagen fibers are composed of bundles of collagen proteins that are cross-linked together (Figure 3). Collagen fibers have a coiled structure, that when stretched becomes uncoiled or straight. This shape explains its non-linear stress strain profile. It takes very little force to uncoil the fiber, but very high levels of force to stretch the fiber when it is uncoiled and completely straight.

The primary purpose of collagen in the healthy myocardium is to prevent overstretch and provide surfaces for the myocytes to attach to in order to aid in transmission of contractile force to the tissue. In healthy tissues, the amount of collagen is very low, but due to disease or aging can become elevated through a process known as fibrosis (41, 58, 94, 211). An excess of collagen fibers increases the stiffness of the tissue which reduces the ability of the LV to fill with blood (115, 121). This can be pictured on the pressure volume diagram as an increase in the slope of the EDPVR, which serves to reduce stroke volume. A severe reduction in ventricle function due to impaired filling is termed diastolic heart failure and is a significant clinical problem. Crosslinking of the collagen network, which is largely controlled by the protein lysyl oxidase has been shown to alter the mechanics of myocardial tissue as well (121, 220).

Elastin is another structural protein that is often overlooked when discussing the mechanical properties of the myocardium. Similar to collagen, elastin forms long, thin fibers. These fibers are termed elastic fibers and consist of an elastin core surrounded by a class of proteins termed microfibrils (173). Microfibrils, such as fibulins and fibrillins play an important role in the assembly of the elastic network, contribute to the mechanical properties of the fibers and provide integrin binding sites (196). Elastic fibers, as their name would indicate have an elastic stress-strain behavior, similar to the mechanical properties of titin, which is much more abundant in the healthy myocardium (48, 118). Studies of elastin in the healthy myocardium remain very limited, however elastin is becoming a more active subject of study in left ventricular remodeling and in regenerative medicine which will be discussed later in this review (48, 108, 130, 208).

Proteoglycans serve an important role in regulating the water content of tissues, although little work has been done on understanding their role in the myocardium (48). Proteoglycans contain many negatively charged gylcosaminoglycan (GAG) side chains that attract and retain water molecules (163). The water retained by the GAG side chains can in turn alter the water composition within the collagen and elastic fibers (104). This change in water content can significantly alter the mechanical properties of the tissue by increasing the residual stress and effectively making the tissue stiffer (48, 104). It has been shown that GAG expression varies spatially in arteries corresponding to differences in residual stress at the inner and outer surfaces of the vessel (6). Proteoglycans also play an important role in fibrilogenesis. Work from the lab of Andrew McCulloch has shown that deletion of the genes for the proteoglycans decorin and biglycan leads to variation in collagen fiber ultrastructure and altered tissue mechanics post-myocardial infarction (26, 206). Elevated

levels of the proteoglycan syndecan-1 have been associated with myocardial fibrosis and the development of diastolic heart failure (190).

Mechanical Testing—Mechanical testing of the left ventricle has been a topic of research for more than 150 years. The earliest mechanical tests involved *ex vivo* inflation testing in which the whole LV would be excised from the body and inflated to various volumes and pressures to essentially obtain the EDPVR. Ludwig and Langendorff in the 19th century developed a method of keeping the heart beating in an ex vivo setting which allowed for the determination of the active properties of the tissue as well as full PV loop analysis (228). The Langendorff perfused heart is still commonly employed in the 21st century as a cost effective method for studying pharmaceutical agents, cardiac toxicology, and ischemia (177). The downside to whole heart testing is that it is difficult to accurately quantify the local stresses and strains of the tissue, giving only average properties for the ventricle.

Mechanical testing of small, excised pieces of cardiac tissue allow for the determination of more localized mechanical properties. The earliest tests used uniaxial tensile testing to examine the material properties of papillary muscles (157, 158). To better represent the *in vivo* loading conditions, biaxial mechanical testing was first employed for myocardial tissues in the 1980s (33). The technique in which a flat piece of excised tissue is trimmed, and then pulled in two directions simultaneously allows for accurate quantification of stresses and strains which can be used to determine the anisotropic, non-linear material properties of the myocardial tissue. Slicing the myocardium into several sheets across the thickness, such that each sheet contained myocytes aligned in the same direction allows for calculation of fiber oriented material properties. Having material properties with a localized reference frame is critical in creating highly accurate mathematical models of the LV. Biaxial mechanical studies have also been conducted in which the tissue was subjected to electrical current so that the mechanical properties of the active tissue could be determined. Lin and Yin found a way to tetanize the tissue and conduct biaxial tests so as to measure the contracted mechanical properties (114). Biaxial mechanical testing is still a gold standard in cardiac mechanics testing and has recently been adapted for the study of tissues from small animals including, rats, mice and mole rats (46, 61).

Another newer technique of mechanical testing is isolated myocyte testing. Zile and colleagues isolated cardiomyoctes and seeded them in an agarose gel which was then used in tensile testing (226, 227). They then used a finite element program to estimate the stress on the myocytes and remove the contribution of the gel in the determination of the mechanical properties. Mechanical testing has also been performed on individual myocytes. In these tests, a single myocyte could be subjected to force and the passive and active mechanical properties could be determined (122). Much like isolated whole hearts, isolated individual myocytes offer an excellent platform for studying the effects of pharmaceutical agents making it a commonly employed method in biomechanics studies (17, 78, 161). Moving to even smaller length scales, sarcomeres have been isolated and subjected to mechanical testing (160).

Implantation of sonomicrometer crystals onto the myocardium of live animals has been used as a means of estimating local in vivo stresses and strains (46). This invasive analysis gives

insight that is more detailed than the data that can be collected from the non-invasive imaging studies. Further, this data can prove to be very important in validating new imaging modalities such as strain analysis methods (5, 79, 113).

Constitutive Equations Used to Model the Ventricular Wall—The myocardium is a non-linear, anisotropic, heterogeneous, soft tissue that undergoes large deformation. To appropriately model this behavior the framework of continuum mechanics must be employed. The general constitutive equation used to relate stress and strain is typically

$$\boldsymbol{t}=\frac{2}{J}\boldsymbol{F}\frac{\delta W}{\delta C}\boldsymbol{F}^{T} \quad (4)$$

Where **t** is the Cauchy stress tensor, **F** is the deformation gradient, **J** is the Jacobian of the deformation gradient, **C** is the right Cauchy Green tensor, and W is the strain energy density function. As shown by this equation, the strain energy density function determines the stress-strain relation of tissues. Various material behavior can be captured by choosing different forms of the strain energy density function and fitting the experimental stress and strain data to this form. The most common strain energy density equation form is the Fung-Type exponential equation originally proposed by Y.C. Fung (50).

$$W=\frac{1}{2}c\left(e^{Q}-1\right) \quad (5)$$

Where c is a constant, and Q is an equation chosen so as to best model the anisotropic behavior of the material. One of the simplest forms of Q often chosen for biaxial material testing is

$$Q=b_1{E_x}^2+b_2{E_y}^2+2b_4E_xE_y \quad (6)$$

Where b1-b4 are constants that govern the mechanical behavior of the material and Ex and Ey are the Green strains in the x and y directions respectively. Typically, the x and y directions are chosen to correspond to the circumferential and longitudinal directions of the heart. High values of c in for the constitutive model described by equations 5 and 6 are characteristic of a more elastic tissue while high values for the b parameters denote a more exponential or non-linear stress-strain behavior, perhaps characteristic of a more collagenous tissue. In general, increasing values of the c and b constants represent increased passive tissue stiffness, which reduces diastolic filling. This model is highly simplistic though and doesn't capture the heterogeneous nature of the myocardial tissue which has rotating fiber directions. Thus, an alternate form of Q that is based on the local fiber direction of the myocytes is often employed.

$$Q=b_{ff}{E_{ff}}^2+b_{xx}\left({E_{cc}}^2+{E_{rr}}^2+{E_{cr}}^2+{E_{rc}}^2\right)+b_{fx}\left({E_{fc}}^2+{E_{cf}}^2+{E_{fr}}^2+{E_{rf}}^2\right) \quad (7)$$

Where b_{ff}, b_{xx}, and b_{fx} are material constants and E_{ff}, E_{cc}, E_{rr}, E_{fc}, and E_{cf} are the components of the Green strain tensor with subscripts, f denoting the fiber direction, c, denoting the cross fiber direction, and r denoting the radial direction.

Since myocardial tissue is primarily composed of water, it is often modeled as incompressible. When the assumption of incompressibility is not acceptable, it is common to see the inclusion of a bulk modulus term with equation 5.

$$W=\frac{1}{2}c\left(e^{Q}-1\right)+\frac{1}{2}K(ln\,(J))^{2} \quad (8)$$

Where K is the bulk modulus and J is the jacobian of the deformation gradient. High values of K represent tissue that is highly incompressible.

Recent work has focused on the development of constitutive equations based on the actual cellular and extracellular structure of the left ventricle (202, 203).

Much work has gone into the field of modeling the active contractile forces generated by the myocytes and many different methods for modeling it have been developed. Typically though, the active contractile force is added to the constitutive equation 1 as

$$\boldsymbol{t}=\frac{2}{J}\boldsymbol{F}\frac{\delta W}{\delta C}\boldsymbol{F}^{T}+T\left(\alpha,\left[Ca^{2+}\right]\right)\boldsymbol{m}\otimes\boldsymbol{m} \quad (9)$$

Where T is the active tension developed by the myocyte which is a function of α, the fiber stretch, and $[Ca^{2+}]$ the calcium concentration. The active force is only generated along the direction of the fiber **m**. Through equation 9, the passive mechanical properties and the active mechanical properties become coupled. A form of the calcium dependent tension generation commonly employed in modeling today was proposed by Hunter et al, 1998 (85).

$$T\left(\alpha,\left[Ca^{2+}\right]\right)=\frac{\left[Ca^{2+}\right]^{n}}{\left[Ca^{2+}\right]^{n}+C_{50}^{n}}T_{max}\left(1+\beta\left(\alpha-1\right)\right) \quad (10)$$

Where n is the hill coefficient, typically chosen to be 2, C_{50}^{n} is the calcium concentration at which the tension generated is half maximal when the fiber is unstretched, T_{max} is the maximum tension generated from an unstretched fiber, and β is a parameter that captures the fact that the binding of Ca^{2+} is dependent upon the length of the fiber.

The electromechanics of cardiac contraction is an ongoing field with several new models being proposed over the last decade (103, 143, 162). Many of these models aim to capture much of the heterogeneity of both electrical transmission and sarcomere length, both of which are dependent upon the local stresses of the tissue (27). For an overview of several recent electromechanical models see the review article by Trayanova and Rice (189).

Stress Analysis of the Heart

The classic model to estimate the average wall stress in the LV is the membrane-based Laplace law.

$$p=\frac{T_\theta}{r_\theta}+\frac{T_\varphi}{r_\varphi} \quad (11)$$

Where T and r are wall stress per unit length and the radius of curvature, with subscripts θ and ϕ denote the circumferential direction and the longitudinal (meridional) direction. For uniform wall thickness h, T= t^*h with t and h being the mean stress and wall thickness.

A simplified model is the spherical model. The Law of Laplace for the spherical LV wall becomes:

$$t=\frac{pr}{2h} \quad (12a)$$

Where t is the Cauchy stress in the plane of the wall, P is the pressure inside the ventricle, r is the deformed radius of the ventricle, and h is the thickness of the myocardial wall. This equation may be suitable for roughly estimating the circumferential or longitudinal stresses near the apex of the ventricle.

For mid-ventricular circumferential wall stress, LV is often simplified into a cylindrical model and the Laplace law become

$$t=\frac{pr}{h} \quad (12b)$$

The stress in the longitudinal direction near the mid-ventricle can still be estimated with equation 12a. While this model is a gross simplification of the actual geometry of the LV it is still used today due to its simplicity. Variations used in membrane models include ellipsoid or prolate spheroidal geometries, which more accurately capture the shape of the LV. For thick-walled ventricles, modified equations have been proposed for mean wall stress estimation for the mid-ventricle of prolate spheroid model

$$t_\varphi=\frac{pb}{2h};\quad t_\theta=\frac{pb}{h}\left(1-\frac{b^2}{2a^2}\right) \quad (12c)$$

Where t_φ and t_θ are the stresses in the longitudinal and circumferential directions, and b and a are the minor and major radii. The choice of equation for stress estimation largely depends on the location of interest, the shape and dimensions of the LV, and the accuracy needed. For example, stresses at the mid-ventricle, or near the base may best be calculated using the equations for the cylindrical shape (equation 12a for the longitudinal direction and equation

12b for the circumferential direction), while stresses near the apex may be better approximated using equation 12a for both directions. If the long axis and short axis dimensions are known, equation 12c will give even better estimates.

For even more accurate analysis of ventricular wall stress, finite element analysis (FEA) is the best choice for accurate stress analysis. Finite element analysis is now the method of choice for conducting accurate stress analyses. Geometries can be accurately imported and digitized from CT, or MRI images allowing for the analysis to be conducted for individual patients. Image based finite element models have been used more and more for patient specific stress analysis (55, 62, 199).

Interestingly, the existence of residual stress significantly reduces the stress concentration in the lumen wall and uniformalizes the stress across the wall thickness (49, 146). While the ventricle is a thick-walled structure, it has been shown that the Laplace law gives a reasonable well estimation of the mean wall stress as compared to the complex models using finite element analysis (138, 223). However, when considering the irregular LV structure and wall thickness variations, especially in MI, FEA is necessary to determine the local wall stress (223).

Biomechanics of Cardiac Function Post-MI

Myocardial infarction (MI) occurs when coronary arteries are blocked by atherosclerostic plaques resulting in the death of cardiac myocytes due to ischemia. Coronary heart disease obstructs the blood flow to the myocardial tissue. It reduces the ability of the heart to effectively pump blood and leads to a dynamic wound healing process that alters the mechanics of the LV as well as the mechanical properties of the myocardial tissue.

Current treatment for myocardial infarction consists of a combination of reperfussion surgery which may consist of arterial grafting or angioplasty and stenting of the artherosclerotic arteries, treatment with pharmaceutical anticoagulants, and anti-thrombotics, as well as long term management of diet and blood pressure often including the use of ACE inhibitors and beta blockers (209).

The Wound Healing Response to MI

MI triggers a complex dynamic wound healing process marked initially by inflammatory processes followed by fibrosis and scar formation. An excellent 2005 review by Holmes, Borg, and Covell breaks down both these changes over the course of the wound healing response in terrific detail (83).

The wound healing response can be broken down into four temporal phases based upon the biological changes occurring at the time. The first phase is the acute ischemic phase which lasts for around the first four to six hours following occlusion of the coronary artery. During this period, the contractile ability of the myocardial tissue in the ischemic region is significantly reduced or eliminated altogether. During this time period, a thinning of the infarct region occurs which results in a right shift of the EDPVR, as well as the ESPVR. This shift reduces the EF of the LV. The infarct region itself, has been shown to become

slightly more compliant than normal during the first hour after myocardial infarction, but actually increases in stiffness by four hours after occlusion. It is theorized that this early increase in stiffness is due to edema in the ischemic region.

The necrotic phase follows the acute ischemic phase and lasts for around 5-7 days. During this phase, inflammation and necrosis set in and clear the injured myocytes and begin to destroy the existing collagen network. The infarct region continues to thin further contributing to dilation of the LV chamber. During this time period the unstressed length of the infarct region appears to become elongated while the end-diastolic lengths appear to be similar to the pre-occlusion state indicating a tissue that has become stiffer. The increase in unstressed length is likely due to the destruction of titin in the infarct region by macrophages and neutrophils. Since this phase of wound healing occurs before new ECM is produced, the increase in stiffness has again been attributed to edema. One of the major complications seen during this time period is rupture of the infarct wall which results from degradation of the structural proteins of the myocardium (11, 54).

The third phase of the wound healing process is the fibrotic phase during which the production of new ECM begins. This period lasts for roughly two to three weeks following the end of the necrotic phase. The fibrotic phase begins with the initial production of a temporary ECM network composed of proteins such as fibronectin and collagen III, which serves as scaffolding for the assembly of stiffer collagen I networks. While, some thinning and elongation of the infarct region still occurs during the early part of the fibrotic phase, the primary mechanical change is an increase in the stiffness of the infarct, especially along the circumferential direction of the LV matching the principal direction of collagen fiber alignment. The increase in stiffness during the fibrotic phase reduces diastolic filling and can in turn lower the ability of the neighboring healthy tissues to contract through the Frank-Starling mechanism (195).

The final phase is referred to as the remodeling phase. During this phase the scar begins to shrink as it becomes a more mature stable structure. During this phase, collagen density alone is no longer the principal determinant of the infarct mechanical properties. Collagen cross-linking increases greatly during this time period which may aid in scar contraction. Interestingly though the literature is divided on whether the infarct tissue becomes stiffer or more compliant during this time period (46, 65). While in general the remodeling phase may be marked by improved LV function, the changes are highly variable from patient to patient and may be dependent upon several factors. When remodeling leads to complications for the patient it is often referred to as adverse LV remodeling, an area of great research interest. A pictorial overview of LV dilation and fibrosis during the first 28 days post-MI in a mouse model adapted from the work of Zamilpa and Lindsey is presented in Figure 4 (221).

Variation in MI Outcome

Since heart failure following MI is primarily the result of mechanical failures, it is important to understand what variations in the remodeling process lead to these various failures. As mentioned earlier, the most catastrophic complication is rupture of the infarct wall. It has been shown in mice that increased infarct size increases the chances of cardiac rupture, and that male mice are 2-3 times more likely to experience rupture (53, 54). The level of

inflammation in the LV also contributes to the risk of cardiac rupture, and the deletion of several inflammatory genes has been shown to reduce the chances of rupture including, MMP-2, MMP-9, and periostin (37, 54, 74, 176). Deletion of the gene for MMP-28 has recently been shown to increase the rate of rupture (124). A comprehensive listing of demographic, clinical presentation, and treatment risk factors for the development of rupture is presented in a 2010 report by Lopez-Sendon et al (120). In their report, they found that the average age of patients who experienced rupture was 74 compared to an average age of 66 for the non-rupture cohort. They also found that 49% of the rupture group was female, while only 33% of the non-rupture group was female, which is an opposite trend from that reported in mice. Patients who experienced cardiac rupture also had lower body weights, were less likely to be smokers, had a reduced incidence of hyperlipidaemia, and were less likely to have had previous cardiovascular events. Diabetes and hypertension were not found to be risk factors. On presentation, patients who went on to experience cardiac rupture were more likely to have ST segment elevation, have reduced systolic blood pressures, and have an increased pulse. Patients who experienced cardiac rupture were also less likely to have been treated with ACE inhibitors, aspirin, thienoppyridine, beta blockers, or statins within the first 24 hours of treatment. Cardiac rupture patients were also more likely to have received thrombolytic treatment, but on average the rupture group was given this treatment at later timepoints following the onset of symptoms.

The development of diastolic heart failure occurs as the result of excessive infarct stiffness preventing the LV from filling. Thus factors that control fibrosis and long term remodeling are also factors in the development of diastolic heart failure. Again, factors such as age, and sex influence the development of heart failure again with women and the elderly being at higher risk (38, 40). Diabetes, which increases LV remodeling, has also been shown to increase the risk for developing diastolic heart failure (3). Increased heart rate and hypertension can also contribute to the risk of developing diastolic heart failure (210).

Systolic heart failure following MI can occur due to the loss of contractile function or can occur as the result of an infarct that is too compliant which can result in infarct bulging (83). LV dilation which increases the load against which the already compromised myocardium must contract worsens the situation. The risk for developing systolic heart failure following myocardial infarction is again associated with age as well as the presence of previous cardiovascular disease, reduced medical intervention and infarct size (133, 187). Interestingly, the risk factors that predict mortality due to systolic heart failure following MI are often reversed, with males and patients with low blood pressure being more likely to die (187). Infarcts located near the apex of the heart were also found to increase the mortality rate (187)

Clearly, there are many factors that play a role in regulating patient outcome post-MI, however many of these factors interact with each other complicating our understanding of the disease progression. A summary of the various factors that contribute to patient outcome are listed in Table 4. Much more research is needed to fully understand the biological causes for the variability in patient outcome.

Role of Mechanical Stress in LV Remodeling and Outcome

The fibrotic and remodeling phases of the MI response are dominated by the production of new ECM proteins. The organization, composition, and assembly of the new ECM material determine the mechanical properties of the tissue which in turn alter the distribution of stress in the tissue as well cardiac function (84). However, the tissue stresses also regulate the production of the new ECM materials in a sort of feedback mechanism (Figure 5). This mechanical feedback system can lead either to the eventual stability of the scar and cardiac function or a progressive deterioration of ventricular function leading to heart failure, referred to as adverse LV remodeling (2). Thus it is important to understand the role that stress plays in regulating the remodeling process.

Mechanical stress leads to deformation of both cells and the ECM which can trigger biological responses through mechanotransduction. Mechanotransduction occurs through several different pathways including the opening of stretch activated ion channels, changes in integrin tension and signaling, the release of proteins from the extracellular matrix, the turnover of intracellular fibers such as actin, the exposure of “hidden” binding domains on cell surface proteins, and changes in spatial chemical gradients (14, 39). Several signaling pathways have been identified as being mechanosensative, including focal adhesion kinases (FAKs) and mitogen activated kinases (MAPKs) such as c-jun N terminal kinase (JNK) and extracellular related kinase (ERK) (39). For an excellent review of mechnotransduction signaling in fibrosis please refer to the 2014 article by Duscher et al (39). For the most part mechanotransudction allows for tissues to modulate their stiffness in order to maintain a mechanical homeostasis. Stress is thought to be a very important factor in the development of the cardiac structure, leading to the helical rotation of the cardiomyocytes as well as the presence of residual stress to balance the total stress across the myocardial wall (181, 188).

In the post-MI environment, the LV has undergone major changes in geometry, including wall thinning and chamber dilation which greatly increase the tissue stresses, especially in the infarct region and border zones (63). The role of mechanical stress in the inflammatory response to MI has not been particularly well studied. Recent work on vascular smooth muscle cells has shown that mechanical stretch increased the levels of both MMP-2 and monocyte chemoattractant protein-1 (214). MMP-13 and ADAMTS-5 both increase in response to mechanical stretch in chondrocytes (184). A study on human foreskin fibroblasts concluded that mechanical stretch does not alter the expression of MMPs but the presence of fibronectin and collagen I does (222). Recent work on rabbit corneal fibroblasts has shown that 5% equibiaxial cyclic stretch results in decreased expression of MMP-2 with a corresponding increase in TIMP-2, while 15% equibiaxial cyclic stretch lead to increased levels of MMP-2 and decreased levels of TIMP-2 (119).

Macrophages play a critical role in the inflammatory response to MI, and these cells are also affected by biomechanical cues (102, 135). Increased stretch of atrial myocytes has been shown to stimulate the recruitment of macrophages (145). The elasticity of macrophages and the mechanical properties of the culture substrate have been shown to alter macrophage function, having effects on phagocytosis, TNF-α production, and altering the transcriptomic profile (150). Further, it was recently shown that elongation of macrophage cell shape, resulted in a transition from the M1 (proinflammatory macrophage phenotype) to the M2

(wound healing macrophage phenotype) (135). Transition to the M2 phenotype has been associated with improved cardiac outcomes post MI (124, 212). Hypoxia has been shown to reduce the ability of macrophages to change their shape and orientation in response to mechanical stretch (148). Much more work is needed to fully understand the contributions of mechanics to the MI inflammatory response.

Neutrophils are another class of leukocytes that play an important role in the inflammatory process post-MI (2, 98). Only a minimal amount of research into mechanotransduction signaling in neutrophils has been conducted, but it has been shown that neutrophils are capable of measuring substrate stiffness and more readily respond to chemotactic gradients when cultured on stiff substrates (87). The proposed mechanism underlying this mechanosensing is by integrin tension. In the blood stream, fluid shear stress has been shown to activate neutrophils and regulate their morphology through G-protein signaling (126, 127). Neutrophils are also producers of MMP-9 which they produce to traverse the basement membrane of tissues and both MMP-2 and MMP-9 have been shown to be upregulated due to increased mechanical stresses in arteries (20, 97). However, it has not been demonstrated that production of MMPs by neutrophils is mechanosensitive.

The role of mechanics in the regulation of the fibrotic process is better understood. Uniaxial mechanical stretch has been shown to increase the ratio of collagen I to collagen III produced by cardiac fibroblasts in culture (29). Cardiac fibroblasts grown under 3% equibiaxial stretch showed an increase in collagen III deposition while those grown under 6% equibiaxial stretch showed decreases in collagen III (105). Mechanical stretch also modulates the production of cyotkines, growth factors, and receptors by cardiac fibroblasts including the production of TGF-β, TNF-α, and angiotensin II receptors as well as their release from the ECM (128, 192, 201). Further, mechanical stress was shown to regulate the transition from fibroblast to myofibroblast, partially by altering the phosphorylation of syndecan-4 (77).

Perhaps most interestingly, mechanical stress and stretch is the primary determinant of collagen organization and alignment in the post-MI environment (47). Fibroblasts have been shown to elongate under stretch and have been shown to orient themselves in the direction of uniaxial stretch in vitro and are thought to orient themselves according to the directions of the principal stretches in vivo (72, 73). Fibroblasts deposit new collagen fibers aligned along the long axis of the cells, and can reorient existing collagen fibers so that they more closely align with the orientation of the cells by establishing focal adhesions that run perpendicular to the direction of stretch (28, 155). The alignment of the collagen fibers not only regulates the anisotropy of the tissue, but it can also impact the migration of other cells through the ECM. A recent study by the Holmes laboratory demonstrated the influence of scar shape and location on collagen formation post-MI in a rat model (47). Their results indicated that the location of the shape of the scar had little effect on the orientation of the collagen fibers, but the location of the scar played a major influence. Collagen was found to be randomly aligned in scars near the apex of the heart where the stresses are nearly uniform in both the longitudinal and circumferential directions. However, scars that were located nearer to the base of the LV had fibers aligned primarily in the circumferential direction. The circumferential direction is the direction of the largest principal stress in the more cylindrical

basal region. Another interesting finding from this study is that the alignment of the existing ECM matrix did not have a major effect on the final ECM matrix three weeks post-MI.

Mechanical regulation of the post-MI wound healing response has also been studied with the use of computational models. Rouillard and Holmes developed an agent based computational model to examine the effects of infarct shape, mechanical stretch, and existing ECM structure on the migration of cardiac fibroblasts and the deposition and alignment of new collagen fibrils (165). They found that the effect of infarct shape had a minimal effect on cell alignment but that the direction of stretch played a major role in the development of an oriented collagen network, matching their experimental results. They also noted that chemical guidance of fibroblasts by chemokine gradients did not play a major role in determining the organization of collagen fibers, but did have an effect on the fibers near the border zones where the gradients are large. This modeling study was recently expanded to a finite element coupled model so as to better capture the mechanical loads imparted on the LV (164). Again the results of the computational model correlated with the experimental findings. Furthermore, the model predicted that fibroblast alignment in the direction of the largest principal stretch acts as a negative feedback mechanism that reduces scar anisotropy since increased fiber deposition in the direction of principal stretch reduces that stretch. Further, they showed that structural guidance cues act as a positive feedback mechanism, and in the absence of mechanical feedback would lead to isotropic scar formation, indicating the importance of biomechanics in regulating the remodeling response. While the paper by Rouillard and Holmes offers a nice multi-scale look at the remodeling process, more work is needed, especially in understanding the interaction between the inflammatory and remodeling responses. Computational models such as the cellular interaction models by Jin and colleagues could be extended to include the role of mechanical regulation (90, 217).

Mechanical Models to predict LVEF

We have previously discussed the use of mechanical modeling in stress analysis and LV remodeling, but perhaps most importantly they can be used to predict cardiac function specifically left ventricular EF. Mechanical modeling allows the researcher to readily change model parameters to study the effects of various pathologies and treatments on cardiac function which may otherwise be difficult and costly to study in the lab.

LVEF is one of the most important determinants of long-term prognosis for patients with coronary artery disease (18). Improving cardiac function as indicated by the LVEF is the major goal of coronary revascularization (angioplasty or bypass grafting) although improvement in patient’s symptoms, such as relief of angina pectoris is also important (86).

A pioneering study by Bogen et al, in 1980 used a membrane model to analyze both the systolic and diastolic behavior of the LV post-MI (16). They were able to vary parameters including the size and stiffness of the infarct region. They found that large and compliant infarcts led to lower cardiac performance than more rigid ones. They also identified the presence of large stresses in the border zone regions and a coupling between the mechanical properties of the infarct tissue and the contractile ability of the healthy tissue. In a follow up paper, Bogen et al, used their computational model to study the effect of varying the

inotropic state of the contractile tissue, establishing the use of computational modeling to simulate potential therapeutic interventions (15).

Simple membrane models were developed to predict LVEF based on cine MRI from clinical patients (70, 147). The model predicted the post-revascularization LVEF at a very good accuracy. Clinical studies have shown that the dysfunctional myocardium can be either irreversible, as infarcted myocardium, or reversible, as hibernating myocardium, with only the hibernating myocardium potentially able to recover its function once reperfused through revascularization (18). The model estimated the LVEF based on the size and properties of the myocardium measured from cine MR images, prior to revascularization (Figure 6). Thus the model could be used to predict the benefit of the procedure and patient outcome. Later, the model was modified to predict LVEF based on patient echocardiographic images (67-69). Since clinical reports have shown that not all patients benefit from revascularization, prediction of the post-revascularization LVEF would be useful in selecting patients for effective revascularization (18). This will help to eliminate non-beneficial revascularization procedures to reduce patient risks of morbidity and mortality and save patient and medical care cost.

Guccione and colleagues developed a finite element model of an ovine LV with aneurysm based on MRI images (63). They used their model primarily to look at border zone dysfunction, and the role of infarct stiffness. They determined that border zone dysfunction was the result of changes in contractility in the region rather than increased levels of stress. This work has since been extended in several studies that aim to establish whether surgical intervention such as the Dor procedure can improve border zone contractility and restore cardiac function (142, 198, 207). A recent study by Warwick et al, developed a model to determine what patients would benefit from surgical repair of LV aneurysms or dilated cardiomyopathy, highlighting the potential utility of computational modeling in the clinical setting (204).

Several finite element models have been developed to study the effect of altering the mechanical properties of the infarct region by therapeutic intervention. Fomovsky et al created a model to examine the influence of scar anisotropy on ejection fraction and found that increasing the longitudinal stiffness of the infarct region would improve cardiac function (44). Kortsmit et al, examined the effect of an injectable hydrogel on the mechanics of the infarct region and on cardiac function (99). They found that the presence of the hydrogel did improve cardiac function.

Voorhees and Han developed a cylindrical LV model to study the influence of collagen alignment, density, and mechanics within the infarct region on cardiac function (195). They concluded that a longitudinal alignment of fibers maximizes EF in the post-MI environment by allowing for increased diastolic filling and increasing contractility through the Frank-Starling mechanism.

A recent study by Wall et al developed a computational model of the post-MI LV that included electromechanical coupling (199). Electrical conduction in the infarct region is significantly altered compared to the healthy tissue and understanding the influence of

electrical conduction on both tissue mechanics and cardiac function will be important in developing new treatments for MI.

Mechanics of MI Treatment

Biomechanics is already playing a major role in the development of new treatments for MI. The use of mesh wrapping placed around the LV has been investigated as a means of reinforcing the infarct tissue and preventing LV dilation (13, 95). The procedure is highly invasive though, and many researchers are instead attempting to increase the stiffness of the infarct tissue directly through the injection of a wide range of hydrogels and tissue fillers (57). These techniques have been shown to prevent LV dilation and reduce adverse remodeling by reducing the mechanical stresses. One interesting approach is the injection of elastin into the infarct area which also shows promise in preventing LV remodeling (139). A more recent study injected stem cells programmed to overexpress elastin into the infarct area and produced very promising results (108). Based on the findings of their computational model, Fomovsky et al, implanted an anisotropic patch over the infarct region of a canine LV and found that the patch did improve systolic function without impairing diastolic function (45). The Cardiokinetix Parachute is a catheter delivered device that expands in the LV and partitions the healthy and infracted segments of the LV, and reduces the mechanical stresses in the myofibers of the healthy region, reducing the risk of developing of hypertrophy (106).

Cardiac mechanics are also important in the development of surgical techniques designed to restore LV function. The Dor procedure in which the ischemic region of the LV is removed and the ventricle then patched so that the final size and geometry roughly match that of the healthy LV has been used for almost 30 years with success (34, 36). Part of the theory behind why this procedure works is that it reduces the mechanical stresses on the LV. The development of accurate, patient specific computational models can further aid improvements in surgical techniques (100, 223).

Left ventricular assist devices (LVADs) are currently used as a short term bridge to transplant in patients with heart failure, including heart failure due to MI (51). Recent advances in the technology are making LVADs a viable long term destination therapy (9, 111, 112, 213). Clearly, a knowledge of mechanical engineering is needed to design and build these pumps, but it is also important to understand the ways in which LVADs alter the mechanics of the heart. LVADs modulate the wall stresses in the myocardial tissue, but also the flow patterns of the blood through the heart and into the aorta which can lead to clinical complications (21, 88) LVADs decrease the filling pressure and mechanical load on the ventricle which can reduce adverse remodeling (51). It has been shown that LVAD devices can reduce the expression of MMP-1 and MMP-9, increase the expression of TIMP-1 and TIMP-3, and decrease the expression of NF-κB (59, 109), Further, LVAD therapy has been shown to prevent myocyte hypertrophy (8). Current state of the art technology has led to the development of continuous flow LVAD devices which improve patient outcome following implantation (25). The decision on what patients should receive LVAD devices is a difficult one, and biomechanical analyses may be able to aid in the decision making process (123).

Pharmaceutical agents are a major part of the treatment regimen for MI, and many of these agents have effects on blood pressure and the remodeling process which can change the

mechanical stresses and deformations of the ventricle wall, altering remodeling (110, 149). Voorhees et al recently showed that deletion of the gene for MMP-9 altered the mechanical properties of the infarct region 7 days post-MI creating a tissue that with increased stiffness (194). The development of computational models focusing on biological and mechanical interaction will be very important in predicting the effects a pharmaceutical agent on both changes in mechanical properties due to remodeling but also in predicting changes in LV function.

The ultimate goal in treatment of myocardial infarction is the generation of new myocardium to replace the dysfunctional myocardium. Advances in regenerative medicine and tissue engineering are making this a possibility. To date, several clinical studies have been performed in which stem cells of various types were delivered to the ischemic myocardium (153). However, there is little evidence in humans that these cells actually differentiated into myocytes. It is known that the differentiation of stem cells into cardiomyocytes is highly regulated by chemical signals such as growth factors and cytokines, electrical signals, and mechanical signals (200). Given the interplay of all these factors, the success of regenerative therapies will likely lie in controlling the mechanical environment of the LV.

Biomechanics in LV hypertrophy and Diastolic Heart Failure

While atherosclerosis in the coronary artery can lead to MI, increased LV pressure due to hypertension, aortic valve stenosis, or stiffening of the arterial walls can lead to LV hypertrophy and diastolic dysfunction. Diastolic heart failure, or heart failure with preserved ejection fraction (HFpEF) has become increasingly studied and is responsible for half of all heart failure hospitalizations (7, 152, 210, 216). Risk factors for HFpEF include aging, diabetes, obesity, and hypertension, and HFpEF has a higher prevalence in women than men.

Patients with HFpEF commonly have an elevated end-diastolic LV pressure as a result of impaired diastolic filling. Aortic valve stenosis reduces the outlet diameter from the ventricle and in turn increases the LV pressures (218). Similarly, peripheral artery stiffening increases the resistance of the circulatory system leading to hypertension and increased LV pressure (215). HFpEF hearts commonly show concentric remodeling characterized by normal LV volume, increased LV mass (thus decreased volume to mass ratio), increased wall thickness, and increased chamber and myocardial stiffness (7). HFpEF hearts undergo hypertrophy with a marked increase in fibrosis, which leads to increased wall stiffness. In fact, it has been shown that both extracellular matrix (MMP, collagen, fibronectin) and titin are altered (117). The increase in wall stiffness prevents both diastolic filling and relaxation. Biomechanically, HFpEF results in a upward and rightward shift of the diastolic pressure-volume curve (225). This means that a high pressure is required to generate a given filling volume.

Diagnosis of HFpEF is often difficult given that there is no change in EF. The current consensus is that diagnosis should be based on either invasive hemodynamic measurements such as LV end-diastolic pressure, mean pulmonary capillary wedge pressure, and τ, or on a combination of tissue Doppler measurements, such as E/e', and biomarkers such as brain

natriuretic peptide (152). It was recently shown strain as measured by speckle tracking echocardiograpy is a predictor of HFpEF patient outcome (178)

Similar to what we have discussed for post-MI remodeling, mechanical stress also plays an important role in the remodeling process that leads to diastolic heart failure. In an early computational model, Segers et al, showed that increased diastolic pressure resulted in LV remodeling that yielded a hypertrophic LV wall (171). Lemmon and Yongathan developed a fluid structure interaction model to examine the role of tissue stiffness on ventricle filling (107). Yang et al, developed a mechanically coupled model of cardiac aging, showing that aging results in increased collagen deposition, increased LV mass, increased LV stiffness, and an increase in LV pressures (217). Many of the models developed so far use simplified geometries, and more work is needed to more fully understand the role of LV tissue properties on the development of HFpEF.

There is currently no proven effective therapy for HFpEF (210). Current treatments aim to control hypertension and heart rate but these therapies cannot reverse remodeling once it has occurred. Several clinical trials have been conducted with minimal success, likely due to the heterogeneity of underlying causes (valve disease, myocyte hypertrophy, fibrosis, atrial fibrillation, etc.) (172). The best outcomes will likely be achieved when therapies are given based on the underlying causes of HFpEF rather than based on the symptoms. Surgery is sometimes an option for treating HFpEF, again depending on the cause of the dysfunction. In general, surgery is not an established option for treating HFpEF, however valve replacement surgery is often prescribed for patients with aortic valve stenosis (218). Understanding the various biomechanical causes of HFpEF will be essential in developing new patient specific therapies and surgical techniques.

Biomechanics of the Right Ventricle, Atria, and Heart Valves

While the focus of this review has been on the cardiac function of the left ventricle, the contributions of the other chambers as well as the function of the valves cannot be discounted.

The right ventricle (RV) of the heart is responsible for pumping blood to the lungs in order to be reoxygenated. While under significantly lower pressures than the LV, the mechanics of the RV are very similar to those of the LV, and RV function can be assessed using many of the same techniques and measurements. Pulmonary hypertension can lead to RV remodeling and the development of RV HF and potentially death (52) A recent article from the Sacks lab, examined the changes in mechanical properties and tissue structure that occur in the RV as a result of pressure overload (81). For a review RV mechanics and function, the reader is directed to the report by the National Heart, Lung, and Blood Institute Working Group on Cellular and Molecular Mechanisms of Right Heart Failure (193).

The atria of the heart are responsible for the filling of the ventricles, and play an important role in cardiac function. Remodeling of the atria is associated with a dilation and stiffening of the chamber similar to that seen in the ventricles and is associated with the development of heart failure (96, 191). These conditions reduce the ability of the atria to fill with blood

and act as a reservoir for ventricle filling (82). It has been experimentally shown that the motion of the ventricle during systole alters the dimensions of the atria changing its reservoir capacity, and that changes in the stiffness of the ventricle alters atrial function as well (10). Improving our understanding of atrial mechanics could aid in the development of treatments for diastolic heart failure. For a discussion of atrial mechanics the reader is directed to the review by Vieira et al (191)

There is a tremendous literature on the biomechanics of normal and diseased heart valves. Heart valves remodel in response to both fluid shear stresses and tissue stresses which has effects on both cell and ECM organization and density (24, 136). Increased valve stiffness has been associated with diseases such as aortic valve stenosis. Treatment of valvular disease is typically achieved through surgery and possibly replacement of the valve, and understanding the complex structure and mechanics of the heart valves will improve both surgical technique and the design of new artificial valves (159). The interested reader may refer to the reviews by Sacks (166, 167).

The development of the heart is a complex biological feat that is largely guided by biomechanical forces. The heart starts as a straight tube and then bends into a loop that will form the basis for the mature heart (180). Torsion is thought to be an important factor in the cardiac looping phenomenon (182). Later in development, hemodynamic factors play a major role in regulating myocyte shape and organization as well as ECM production (125). For overviews of biomechanics in the heart development and growth can refer to the papers by Taber et al and a recent review of the role of mechanotransduction in development by Majkut et al (125, 179-182).

Future Perspectives and Directions

Cardiac biomechanics is a broad field and there are many areas that need further study. The following are some of the most pressing issues in the field: 1. We need better constitutive models for myocardial tissue, ideally models that include the effects of cellular proteins like titin, 2. We need improved multi-scale, whole-heart models of cardiac behavior that include the electrical, chemical, cellular, and mechanical factors, 3. We need to further study the role of mechanical stress in the inflammatory period and develop computational models that include this effect in the remodeling process, 4. We need to examine how deletion or over expression of individual genes affects tissue mechanics, 5. We need to use the principles of mechanical analysis to develop effective treatments for diastolic heart failure. Biomechanical analysis will allow us to address these knowledge gaps and improve the way we diagnose and treat future patients.

Conclusion

Biomechanical factors are the primary determinants of cardiac function in both the normal and diseased heart. The mechanical properties of cardiac tissue alter the ability of the ventricles and atria to fill with blood and contract. Biological processes such as inflammation and fibrosis have a direct impact on tissue mechanics and alterations to the local mechanical stresses drive adverse remodeling and contribute to the development heart

failure. Recognition of the important role that biomechanics plays in regulating heart function has led to mechanical measures such as tissue strain being used to diagnose cardiac disease. Mechanical stress analysis can allow physicians to determine what patients may benefit from surgical intervention.

Acknowledgements

This work was supported by grant HL095852 and HHSN 268201000036C (N01-HV-00244) for the San Antonio Cardiovascular Proteomics Center from the National Institutes of Health.

References

1. Amundsen BH, Helle-Valle T, Edvardsen T, Torp H, Crosby J, Lyseggen E, Støylen A, Ihlen H, Lima JAC, Smiseth OA, Slørdahl SA. Noninvasive Myocardial Strain Measurement by Speckle Tracking Echocardiography: Validation Against Sonomicrometry and Tagged Magnetic Resonance Imaging. Journal of the American College of Cardiology. 2006; 47:789–793. [PubMed: 16487846]
2. Anzai T. Post-infarction inflammation and left ventricular remodeling: a double-edged sword. Circ J. 2013; 77:580–587. [PubMed: 23358460]
3. Aronson D, Musallam A, Lessick J, Dabbah S, Carasso S, Hammerman H, Reisner S, Agmon Y, Mutlak D. Impact of diastolic dysfunction on the development of heart failure in diabetic patients after acute myocardial infarction. Circ Heart Fail. 2010; 3:125–131. [PubMed: 19910536]
4. Ashikaga, H.; Criscione, JC.; Omens, JH.; Covell, JW.; Ingels, NB. Transmural left ventricular mechanics underlying torsional recoil during relaxation. 2004.
5. Ashraf M, Myronenko A, Nguyen T, Inage A, Smith W, Lowe RI, Thiele K, Gibbons Kroeker CA, Tyberg JV, Smallhorn JF, Sahn DJ, Song X. Defining left ventricular apex-to-base twist mechanics computed from high-resolution 3D echocardiography: validation against sonomicrometry. JACC Cardiovasc Imaging. 2010; 3:227–234. [PubMed: 20223418]
6. Azeloglu, EU.; Albro, MB.; Thimmappa, VA.; Ateshian, GA.; Costa, KD. Heterogeneous transmural proteoglycan distribution provides a mechanism for regulating residual stresses in the aorta. 2008.
7. Aziz F, Tk LA, Enweluzo C, Dutta S, Zaeem M. Diastolic heart failure: a concise review. Journal of clinical medicine research. 2013; 5:327–334. [PubMed: 23986796]
8. Baba HA, Stypmann J, Grabellus F, Kirchhof P, Sokoll A, Schafers M, Takeda A, Wilhelm MJ, Scheld HH, Takeda N, Breithardt G, Levkau B. Dynamic regulation of MEK/Erks and Akt/GSK-3beta in human end-stage heart failure after left ventricular mechanical support: myocardial mechanotransduction-sensitivity as a possible molecular mechanism. Cardiovasc Res. 2003; 59:390–399. [PubMed: 12909322]
9. Badiwala MV, Rao V. Left ventricular device as destination therapy: are we there yet? Curr Opin Cardiol. 2009; 24:184–189. [PubMed: 19532106]
10. Barbier P, Solomon SB, Schiller NB, Glantz SA. Left Atrial Relaxation and Left Ventricular Systolic Function Determine Left Atrial Reservoir Function. Circulation. 1999; 100:427–436. [PubMed: 10421605]
11. Becker RC, Gore JM, Lambrew C, Douglas Weaver W, Michael Rubison R, French WJ, Tiefenbrunn AJ, Bowlby LJ, Rogers WJ. A composite view of cardiac rupture in the United States national registry of myocardial infarction. Journal of the American College of Cardiology. 1996; 27:1321–1326. [PubMed: 8626938]
12. Blaudszun G, Morel DR. Relevance of the volume-axis intercept, V0, compared with the slope of end-systolic pressure-volume relationship in response to large variations in inotropy and afterload in rats. Exp Physiol. 2011; 96:1179–1195. [PubMed: 21890525]
13. Blom A, Pilla J, Gorman R, Gorman J, Mukherjee R, Spinale F, Acker M. Infarct Size Reduction and Attenuation of Global Left Ventricular Remodeling with the CorCap™ Cardiac Support Device Following Acute Myocardial Infarction in Sheep. Heart failure reviews. 2005; 10:125–139. [PubMed: 16258720]

14. Boccafoschi F, Mosca C, Ramella M, Valente G, Cannas M. The effect of mechanical strain on soft (cardiovascular) and hard (bone) tissues: common pathways for different biological outcomes. Cell adhesion & migration. 2013; 7:165–173. [PubMed: 23287581]
15. Bogen DK, Needleman A, McMahon TA. An analysis of myocardial infarction. The effect of regional changes in contractility. Circ Res. 1984; 55:805–815. [PubMed: 6499135]
16. Bogen DK, Rabinowitz SA, Needleman A, McMahon TA, Abelmann WH. An analysis of the mechanical disadvantage of myocardial infarction in the canine left ventricle. Circ Res. 1980; 47:728–741. [PubMed: 7418131]
17. Bollensdorff C, Lookin O, Kohl P. Assessment of contractility in intact ventricular cardiomyocytes using the dimensionless 'Frank-Starling Gain' index. Pflügers Archiv. 2011; 462:39–48. [PubMed: 21494804]
18. Bonow RO. The hibernating myocardium: implications for management of congestive heart failure. (Review). The American journal of cardiology. 1995; 75:17A–25A.
19. Borlaug BA, Kass DA. Invasive hemodynamic assessment in heart failure. Cardiology clinics. 2011; 29:269–280. [PubMed: 21459248]
20. Bradley LM, Douglass MF, Chatterjee D, Akira S, Baaten BJG. Matrix Metalloprotease 9 Mediates Neutrophil Migration into the Airways in Response to Influenza Virus-Induced Toll-Like Receptor Signaling. PLoS Pathog. 2012; 8:e1002641. [PubMed: 22496659]
21. Brown AG, Shi Y, Arndt A, Muller J, Lawford P, Hose DR. Importance of realistic LVAD profiles for assisted aortic simulations: evaluation of optimal outflow anastomosis locations. Comput Methods Biomech Biomed Engin. 2012; 15:669–680. [PubMed: 21409657]
22. Buckberg G, Hoffman JIE, Nanda NC, Coghlan C, Saleh S, Athanasuleas C. Ventricular Torsion and Untwisting: Further Insights into Mechanics and Timing Interdependence: A Viewpoint. Echocardiography. 2011; 28:782–804. [PubMed: 21843256]
23. Burns AT, La Gerche A, Prior DL, Macisaac AI. Left ventricular untwisting is an important determinant of early diastolic function. JACC Cardiovascular imaging. 2009; 2:709–716. [PubMed: 19520340]
24. Butcher JT, Penrod AM, García AJ, Nerem RM. Unique Morphology and Focal Adhesion Development of Valvular Endothelial Cells in Static and Fluid Flow Environments. Arteriosclerosis, Thrombosis, and Vascular Biology. 2004; 24:1429–1434.
25. Caccamo M, Eckman P, John R. Current state of ventricular assist devices. Curr Heart Fail Rep. 2011; 8:91–98. [PubMed: 21336538]
26. Campbell PH, Hunt DL, Jones Y, Harwood F, Amiel D, Omens JH, McCulloch AD. Effects of biglycan deficiency on myocardial infarct structure and mechanics. Mol Cell Biomech. 2008; 5:27–35. [PubMed: 18524244]
27. Campbell SG, Flaim SN, Leem CH, McCulloch AD. Mechanisms of transmurally varying myocyte electromechanics in an integrated computational model. Philosophical transactions Series A, Mathematical, physical, and engineering sciences. 2008; 366:3361–3380.
28. Canty EG, Starborg T, Lu Y, Humphries SM, Holmes DF, Meadows RS, Huffman A, O'Toole ET, Kadler KE. Actin filaments are required for fibripositor-mediated collagen fibril alignment in tendon. J Biol Chem. 2006; 281:38592–38598. [PubMed: 17020878]
29. Carver W, Nagpal ML, Nachtigal M, Borg TK, Terracio L. Collagen expression in mechanically stimulated cardiac fibroblasts. Circ Res. 1991; 69:116–122. [PubMed: 2054929]
30. Chang MC, Mondy JS 3rd, Meredith JW, Miller PR, Owings JT, Holcroft JW. Clinical application of ventricular end-systolic elastance and the ventricular pressure-volume diagram. Shock. 1997; 7:413–419. [PubMed: 9185240]
31. Cingolani OH, Kass DA. Pressure-volume relation analysis of mouse ventricular function. American Journal of Physiology - Heart and Circulatory Physiology. 2011; 301:H2198–H2206. [PubMed: 21926344]
32. de Tombe PP, ter Keurs HE. The velocity of cardiac sarcomere shortening: mechanisms and implications. J Muscle Res Cell Motil. 2012; 33:431–437. [PubMed: 22752243]
33. Demer LL, Yin FC. Passive biaxial mechanical properties of isolated canine myocardium. J Physiol. 1983; 339:615–630. [PubMed: 6887039]

34. Di Donato M, Castelvecchio S, Menicanti L. Surgical treatment of ischemic heart failure: the Dor procedure. Circ J. 2009; 73(Suppl A):A1–5. [PubMed: 19474510]
35. Dickstein K, Cohen-Solal A, Filippatos G, McMurray JJV, Ponikowski P, Poole-Wilson PA, Strömberg A, van Veldhuisen DJ, Atar D, Hoes AW, Keren A, Mebazaa A, Nieminen M, Priori SG, Swedberg K, Guidelines ECfP, Vahanian A, Camm J, De Caterina R, Dean V, Dickstein K, Filippatos G, Funck-Brentano C, Hellemans I, Kristensen SD, McGregor K, Sechtem U, Silber S, Tendera M, Widimsky P, Zamorano JL, Reviewers D, Tendera M, Auricchio A, Bax J, Böhm M, Corrà U, della Bella P, Elliott PM, Follath F, Gheorghiade M, Hasin Y, Hernborg A, Jaarsma T, Komajda M, Kornowski R, Piepoli M, Prendergast B, Tavazzi L, Vachiery J-L, Verheugt FWA, Zamorano JL, Zannad F. ESC Guidelines for the diagnosis and treatment of acute and chronic heart failure 2008: The Task Force for the Diagnosis and Treatment of Acute and Chronic Heart Failure 2008 of the European Society of Cardiology. Developed in collaboration with the Heart Failure Association of the ESC (HFA) and endorsed by the European Society of Intensive Care Medicine (ESICM). European Heart Journal. 2008; 29:2388–2442. [PubMed: 18799522]
36. Dor V, Sabatier M, Montiglio F, Civaia F, DiDonato M. Endoventricular patch reconstruction of ischemic failing ventricle. a single center with 20 years experience. advantages of magnetic resonance imaging assessment. Heart failure reviews. 2004; 9:269–286. [PubMed: 15886973]
37. Ducharme A, Frantz S, Aikawa M, Rabkin E, Lindsey M, Rohde LE, Schoen FJ, Kelly RA, Werb Z, Libby P, Lee RT. Targeted deletion of matrix metalloproteinase-9 attenuates left ventricular enlargement and collagen accumulation after experimental myocardial infarction. J Clin Invest. 2000; 106:55–62. [PubMed: 10880048]
38. Dunlay SM, Roger VL. Gender differences in the pathophysiology, clinical presentation, and outcomes of ischemic heart failure. Curr Heart Fail Rep. 2012; 9:267–276. [PubMed: 22864856]
39. Duscher D, Maan ZN, Wong VW, Rennert RC, Januszyk M, Rodrigues M, Hu M, Whitmore AJ, Whittam AJ, Longaker MT, Gurtner GC. Mechanotransduction and fibrosis. J Biomech. 2014; 47:1997–2005. [PubMed: 24709567]
40. Ennezat PV, Lamblin N, Mouquet F, Tricot O, Quandalle P, Aumegeat V, Equine O, Nugue O, Segrestin B, de Groote P, Bauters C. The effect of ageing on cardiac remodelling and hospitalization for heart failure after an inaugural anterior myocardial infarction. Eur Heart J. 2008; 29:1992–1999. [PubMed: 18567671]
41. Fan D, Takawale A, Lee J, Kassiri Z. Cardiac fibroblasts, fibrosis and extracellular matrix remodeling in heart disease. Fibrogenesis Tissue Repair. 2012; 5:15. [PubMed: 22943504]
42. Fann JI, Sarris GE, Ingels NB Jr. Niczyporuk MA, Yun KL, Daughters GT 2nd, Derby GC, Miller DC. Regional epicardial and endocardial two-dimensional finite deformations in canine left ventricle. Am J Physiol. 1991; 261:H1402–1410. [PubMed: 1951727]
43. Foley TA, M SV, Anavekar NS, Bonnichsen CR, Morris MF, Miller TD, Araoz PA. Measuring Left Ventricualar Ejection Fraction - Techniques and Potential Pitfalls. European Cardiology. 2012; 8:108–114.
44. Fomovsky G, Macadangdang J, Ailawadi G, Holmes J. Model-Based Design of Mechanical Therapies for Myocardial Infarction. Journal of cardiovascular translational research. 2011; 4:82–91. [PubMed: 21088945]
45. Fomovsky GM, Clark SA, Parker KM, Ailawadi G, Holmes JW. Anisotropic Reinforcement of Acute Anteroapical Infarcts Improves Pump Function / Clinical Perspective. Circulation: Heart Failure. 2012; 5:515–522. [PubMed: 22665716]
46. Fomovsky GM, Holmes JW. Evolution of scar structure, mechanics, and ventricular function after myocardial infarction in the rat. American Journal of Physiology-Heart and Circulatory Physiology. 2010; 298:H221–H228. [PubMed: 19897714]
47. Fomovsky GM, Rouillard AD, Holmes JW. Regional mechanics determine collagen fiber structure in healing myocardial infarcts. Journal of Molecular and Cellular Cardiology. 2012; 52:1083–1090. [PubMed: 22418281]
48. Fomovsky GM, Thomopoulos S, Holmes JW. Contribution of extracellular matrix to the mechanical properties of the heart. Journal of Molecular and Cellular Cardiology. 2010; 48:490–496. [PubMed: 19686759]
49. Fung, YC. Biomechanics: Circulation. Springer; New York: 1997.

50. Fung, YC. Biomechanics: Mechanical Properties of Living Tissues. Springer; New York: 1993.
51. Gajarsa J, Kloner R. Left ventricular remodeling in the post-infarction heart: a review of cellular, molecular mechanisms, and therapeutic modalities. Heart failure reviews. 2011; 16:13–21. [PubMed: 20623185]
52. Galie N, Hoeper MM, Humbert M, Torbicki A, Vachiery JL, Barbera JA, Beghetti M, Corris P, Gaine S, Gibbs JS, Gomez-Sanchez MA, Jondeau G, Klepetko W, Opitz C, Peacock A, Rubin L, Zellweger M, Simonneau G. Guidelines for the diagnosis and treatment of pulmonary hypertension: the Task Force for the Diagnosis and Treatment of Pulmonary Hypertension of the European Society of Cardiology (ESC) and the European Respiratory Society (ERS), endorsed by the International Society of Heart and Lung Transplantation (ISHLT). Eur Heart J. 2009; 30:2493–2537. [PubMed: 19713419]
53. Gao X-M, Xu Q, Kiriazis H, Dart AM, Du X-J. Mouse model of post-infarct ventricular rupture: time course, strain- and gender-dependency, tensile strength, and histopathology. Cardiovasc Res. 2005; 65:469–477. [PubMed: 15639486]
54. Gao XM, Ming ZQ, Su YD, Fang L, Kiriazis H, Xu Q, Dart AM, Du XJ. Infarct size and post-infarct inflammation determine the risk of cardiac rupture in mice. International Journal of Cardiology. 2010; 143:20–28. [PubMed: 19195725]
55. Ghaemi H, Behdinan K, Spence AD. In vitro technique in estimation of passive mechanical properties of bovine heart Part II. Constitutive relation and finite element analysis. Medical Engineering & Physics. 2009; 31:83–91. [PubMed: 18539073]
56. Gorcsan J 3rd, Tanaka H. Echocardiographic assessment of myocardial strain. J Am Coll Cardiol. 2011; 58:1401–1413. [PubMed: 21939821]
57. Gorman R, Jackson B, Burdick J, Gorman J. Infarct Restraint to Limit Adverse Ventricular Remodeling. Journal of cardiovascular translational research. 2011; 4:73–81. [PubMed: 21161462]
58. Gorman, RC.; Jackson, BM.; Gorman, JH.; Edmunds, LH. The Mechanics of the Fibrosed/Remodeled Heart. In: Villarreal, FJ., editor. Interstitial Fibrosis in Heart Failure. Springer; New York: 2005. p. 149-163.
59. Grabellus F, Levkau B, Sokoll A, Welp H, Schmid C, Deng MC, Takeda A, Breithardt G, Baba HA. Reversible activation of nuclear factor-kappaB in human end-stage heart failure after left ventricular mechanical support. Cardiovasc Res. 2002; 53:124–130. [PubMed: 11744020]
60. Greenbaum RA, Ho SY, Gibson DG, Becker AE, Anderson RH. Left ventricular fibre architecture in man. Br Heart J. 1981; 45:248–263. [PubMed: 7008815]
61. Grimes KM, Voorhees A, Chiao YA, Han HC, Lindsey ML, Buffenstein R. Cardiac function of the naked mole-rat: ecophysiological responses to working underground. Am J Physiol Heart Circ Physiol. 2014; 306:H730–737. [PubMed: 24363308]
62. Guccione JM, Costa KD, McCulloch AD. Finite element stress analysis of left ventricular mechanics in the beating dog heart. J Biomech. 1995; 28:1167–1177. [PubMed: 8550635]
63. Guccione JM, Moonly SM, Moustakidis P, Costa KD, Moulton MJ, Ratcliffe MB, Pasque MK. Mechanism underlying mechanical dysfunction in the border zone of left ventricular aneurysm: a finite element model study. Ann Thorac Surg. 2001; 71:654–662. [PubMed: 11235723]
64. Guerra M, Amorim MJ, Mota JC, Vouga L, Leite-Moreira A. Rationale, design and methodology for Intraventricular Pressure Gradients Study: a novel approach for ventricular filling assessment in normal and falling hearts. Journal of cardiothoracic surgery. 2011; 6:67. [PubMed: 21569272]
65. Gupta KB, Ratcliffe MB, Fallert MA, Edmunds LH Jr. Bogen DK. Changes in passive mechanical stiffness of myocardial tissue with aneurysm formation. Circulation. 1994; 89:2315–2326. [PubMed: 8181158]
66. Halper J. Proteoglycans and diseases of soft tissues. Adv Exp Med Biol. 2014; 802:49–58. [PubMed: 24443020]
67. Han HC. An echocardiogram-based 16-segment model for predicting left ventricular ejection fraction improvement. J Theor Biol. 2004; 228:7–15. [PubMed: 15064079]
68. Han HC, Lerakis S. The relation between viable segments and left ventricular ejection fraction improvement. Journal of medical engineering & technology. 2004; 28:242–253. [PubMed: 15513742]

69. Han HC, Martin RP, Lerakis G, Lerakis S. Prediction of the left ventricular ejection fraction improvement using echocardiography and mechanical modeling. J Am Soc Echocardiogr. 2005; 18:718–721. [PubMed: 16003268]
70. Han HC, Oshinski JN, Ku DN, Pettigrew RI. A left ventricle model to predict post-revascularization ejection fraction based on cine magnetic resonance images. J Biomech Eng. 2002; 124:52–55. [PubMed: 11871605]
71. Hanft LM, Korte FS, McDonald KS. Cardiac function and modulation of sarcomeric function by length. Cardiovascular Research. 2008; 77:627–636. [PubMed: 18079105]
72. Hariton I, deBotton G, Gasser T, Holzapfel G. Stress-driven collagen fiber remodeling in arterial walls. Biomechanics and modeling in mechanobiology. 2007; 6:163–175. [PubMed: 16912884]
73. Haston WS, Shields JM, Wilkinson PC. The orientation of fibroblasts and neutrophils on elastic substrata. Exp Cell Res. 1983; 146:117–126. [PubMed: 6861903]
74. Hayashidani S, Tsutsui H, Ikeuchi M, Shiomi T, Matsusaka H, Kubota T, Imanaka-Yoshida K, Itoh T, Takeshita A. Targeted deletion of MMP-2 attenuates early LV rupture and late remodeling after experimental myocardial infarction. American Journal of Physiology - Heart and Circulatory Physiology. 2003; 285:H1229–H1235. [PubMed: 12775562]
75. Healy LJ, Jiang Y, Hsu EW. Quantitative comparison of myocardial fiber structure between mice, rabbit, and sheep using diffusion tensor cardiovascular magnetic resonance. Journal of cardiovascular magnetic resonance : official journal of the Society for Cardiovascular Magnetic Resonance. 2011; 13:74. [PubMed: 22117695]
76. Hein S, Gaasch WH, Schaper J. Giant Molecule Titin and Myocardial Stiffness. Circulation. 2002; 106:1302–1304. [PubMed: 12221041]
77. Herum KM, Lunde IG, Skrbic B, Florholmen G, Behmen D, Sjaastad I, Carlson CR, Gomez MF, Christensen G. Syndecan-4 signaling via NFAT regulates extracellular matrix production and cardiac myofibroblast differentiation in response to mechanical stress. J Mol Cell Cardiol. 2013; 54:73–81. [PubMed: 23178899]
78. Herzog JA, Leonard TR, Jinha A, Herzog W. Are titin properties reflected in single myofibrils? J Biomech. 2012; 45:1893–1899. [PubMed: 22677335]
79. Heyde B, Bouchez S, Thieren S, Vandenheuvel M, Jasaityte R, Barbosa D, Claus P, Maes F, Wouters P, D'Hooge J. Elastic image registration to quantify 3-D regional myocardial deformation from volumetric ultrasound: experimental validation in an animal model. Ultrasound Med Biol. 2013; 39:1688–1697. [PubMed: 23791543]
80. Hidalgo C, Hudson B, Bogomolovas J, Zhu Y, Anderson B, Greaser M, Labeit S, Granzier H. PKC Phosphorylation of Titin's PEVK Element. Circulation Research. 2009; 105:631–638. [PubMed: 19679839]
81. Hill MR, Simon MA, Valdez-Jasso D, Zhang W, Champion HC, Sacks MS. Structural and Mechanical Adaptations of Right Ventricle Free Wall Myocardium to Pressure Overload. Annals of Biomedical Engineering. 2014
82. Hoit BD, Shao Y, Tsai LM, Patel R, Gabel M, Walsh RA. Altered left atrial compliance after atrial appendectomy. Influence on left atrial and ventricular filling. Circ Res. 1993; 72:167–175. [PubMed: 8417839]
83. Holmes JW, Borg TK, Covell JW. Structure and mechanics of healing myocardial infarcts. Annu Rev Biomed Eng. 2005; 7:223–253. [PubMed: 16004571]
84. Holmes JW, Nunez JA, Covell JW. Functional implications of myocardial scar structure. Am J Physiol Heart Circ Physiol. 1997; 272:H2123–H2130.
85. Hunter PJ, McCulloch AD, ter Keurs HE. Modelling the mechanical properties of cardiac muscle. Progress in biophysics and molecular biology. 1998; 69:289–331. [PubMed: 9785944]
86. Iskandrian AS, Heo J, Schelbert HR. Myocardial viability: methods of assessment and clinical relevance.(Review). Philadelphia Heart Institute, Presbyterian Medical Center, PA 19104, USA. 1996; 132:1226–1235.
87. Jannat RA, Robbins GP, Ricart BG, Dembo M, Hammer DA. Neutrophil adhesion and chemotaxis depend on substrate mechanics. J Phys Condens Matter. 2010; 22:194117. [PubMed: 20473350]

88. Jhun CS, Sun K, Cysyk JP. Continuous flow left ventricular pump support and its effect on regional left ventricular wall stress: finite element analysis study. Medical & biological engineering & computing. 2014

89. Jiang K, Yu X. Quantification of regional myocardial wall motion by cardiovascular magnetic resonance. Quant Imaging Med Surg. 2014; 4:345–357. [PubMed: 25392821]

90. Jin YF, Han HC, Berger J, Dai Q, Lindsey ML. Combining experimental and mathematical modeling to reveal mechanisms of macrophage-dependent left ventricular remodeling. Bmc Systems Biology. 2011:5. [PubMed: 21219666]

91. Kadler K. Matrix loading: Assembly of extracellular matrix collagen fibrils during embryogenesis. Birth Defects Research Part C: Embryo Today: Reviews. 2004; 72:1–11.

92. Kadler KE, Hill A, Canty-Laird EG. Collagen fibrillogenesis: fibronectin, integrins, and minor collagens as organizers and nucleators. Current Opinion in Cell Biology. 2008; 20:495–501. [PubMed: 18640274]

93. Kalogeropoulos AP, Georgiopoulou VV, Gheorghiade M, Butler J. Echocardiographic evaluation of left ventricular structure and function: new modalities and potential applications in clinical trials. J Card Fail. 2012; 18:159–172. [PubMed: 22300785]

94. Kania G, Blyszczuk P, Eriksson U. Mechanisms of Cardiac Fibrosis in Inflammatory Heart Disease. Trends in Cardiovascular Medicine. 2009; 19:247–252. [PubMed: 20447565]

95. Kelley ST, Malekan R, Gorman JH 3rd, Jackson BM, Gorman RC, Suzuki Y, Plappert T, Bogen DK, Sutton MG, Edmunds LH Jr. Restraining infarct expansion preserves left ventricular geometry and function after acute anteroapical infarction. Circulation. 1999; 99:135–142. [PubMed: 9884390]

96. Khan A, Moe GW, Nili N, Rezaei E, Eskandarian M, Butany J, Strauss BH. The cardiac atria are chambers of active remodeling and dynamic collagen turnover during evolving heart failure. Journal of the American College of Cardiology. 2004; 43:68–76. [PubMed: 14715186]

97. Kim YS, Galis ZS, Rachev A, Han HC, Vito RP. Matrix metalloproteinase-2 and -9 are associated with high stresses predicted using a nonlinear heterogeneous model of arteries. Journal of biomechanical engineering. 2009; 131:011009. [PubMed: 19045925]

98. Kolaczkowska E, Kubes P. Neutrophil recruitment and function in health and inflammation. Nat Rev Immunol. 2013; 13:159–175. [PubMed: 23435331]

99. Kortsmit J, Davies NH, Miller R, Macadangdang JR, Zilla P, Franz T. The effect of hydrogel injection on cardiac function and myocardial mechanics in a computational post-infarction model. Comput Methods Biomech Biomed Engin. 2013; 16:1185–1195. [PubMed: 22439799]

100. Krishnamurthy A, Villongco CT, Chuang J, Frank LR, Nigam V, Belezzuoli E, Stark P, Krummen DE, Narayan S, Omens JH, McCulloch AD, Kerckhoffs RC. Patient-Specific Models of Cardiac Biomechanics. J Comput Phys. 2013; 244:4–21. [PubMed: 23729839]

101. Kuznetsova T, Herbots L, Richart T, D'hooge J, Thijs L, Fagard RH, Herregods M-C, Staessen JA. Left ventricular strain and strain rate in a general population. European heart journal. 2008; 29:2014–2023. [PubMed: 18583396]

102. Lambert JM, Lopez EF, Lindsey ML. Macrophage roles following myocardial infarction. International Journal of Cardiology. 2008; 130:147–158. [PubMed: 18656272]

103. Land S, Niederer SA, Aronsen JM, Espe EK, Zhang L, Louch WE, Sjaastad I, Sejersted OM, Smith NP. An analysis of deformation-dependent electromechanical coupling in the mouse heart. The Journal of physiology. 2012; 590:4553–4569. [PubMed: 22615436]

104. Lanir Y. Osmotic swelling and residual stress in cardiovascular tissues. Journal of Biomechanics. 2012; 45:780–789. [PubMed: 22236524]

105. Lee AA, Delhaas T, McCulloch AD, Villarreal FJ. Differential Responses of Adult Cardiac Fibroblasts to in vitro Biaxial Strain Patterns. Journal of Molecular and Cellular Cardiology. 1999; 31:1833–1843. [PubMed: 10525421]

106. Lee LC, Ge L, Zhang Z, Pease M, Nikolic SD, Mishra R, Ratcliffe MB, Guccione JM. Patient-specific finite element modeling of the Cardiokinetix Parachute((R)) device: effects on left ventricular wall stress and function. Med Biol Eng Comput. 2014; 52:557–566. [PubMed: 24793158]

107. Lemmon JD, Yoganathan AP. Computational modeling of left heart diastolic function: examination of ventricular dysfunction. J Biomech Eng. 2000; 122:297–303. [PubMed: 11036551]
108. Li S-H, Sun Z, Guo L, Han M, Wood MFG, Ghosh N, Alex Vitkin I, Weisel RD, Li R-K. Elastin overexpression by cell-based gene therapy preserves matrix and prevents cardiac dilation. Journal of Cellular and Molecular Medicine. 2012; 16:2429–2439. [PubMed: 22435995]
109. Li YY, Feng Y, McTiernan CF, Pei W, Moravec CS, Wang P, Rosenblum W, Kormos RL, Feldman AM. Downregulation of matrix metalloproteinases and reduction in collagen damage in the failing human heart after support with left ventricular assist devices. Circulation. 2001; 104:1147–1152. [PubMed: 11535571]
110. Liang CS, Gavras H, Black J, Sherman LG, Hood WB Jr. Renin-angiotensin system inhibition in acute myocardial infarction in dogs. Effects on systemic hemodynamics, myocardial blood flow, segmental myocardial function and infarct size. Circulation. 1982; 66:1249–1255. [PubMed: 6183019]
111. Lietz K, Miller LW. Left ventricular assist devices: evolving devices and indications for use in ischemic heart disease. Curr Opin Cardiol. 2004; 19:613–618. [PubMed: 15502508]
112. Lietz K, Miller LW. Will left-ventricular assist device therapy replace heart transplantation in the foreseeable future? Curr Opin Cardiol. 2005; 20:132–137. [PubMed: 15711200]
113. Lima JA, Jeremy R, Guier W, Bouton S, Zerhouni EA, McVeigh E, Buchalter MB, Weisfeldt ML, Shapiro EP, Weiss JL. Accurate systolic wall thickening by nuclear magnetic resonance imaging with tissue tagging: correlation with sonomicrometers in normal and ischemic myocardium. J Am Coll Cardiol. 1993; 21:1741–1751. [PubMed: 8496547]
114. Lin DH, Yin FC. A multiaxial constitutive law for mammalian left ventricular myocardium in steady-state barium contracture or tetanus. Journal of biomechanical engineering. 1998; 120:504–517. [PubMed: 10412422]
115. Lin J, Lopez EF, Jin Y, Van Remmen H, Bauch T, Han HC, Lindsey ML. Age-related cardiac muscle sarcopenia: Combining experimental and mathematical modeling to identify mechanisms. Experimental gerontology. 2008; 43:296–306. [PubMed: 18221848]
116. Linke WA. Sense and stretchability: The role of titin and titin-associated proteins in myocardial stress-sensing and mechanical dysfunction. Cardiovascular Research. 2008; 77:637–648. [PubMed: 17475230]
117. Linke WA, Hamdani N. Gigantic business: titin properties and function through thick and thin. Circ Res. 2014; 114:1052–1068. [PubMed: 24625729]
118. Linke WA, Popov VI, Pollack GH. Passive and active tension in single cardiac myofibrils. Biophys J. 1994; 67:782–792. [PubMed: 7948691]
119. Liu C, Feng P, Li X, Song J, Chen W. Expression of MMP-2, MT1-MMP, and TIMP-2 by cultured rabbit corneal fibroblasts under mechanical stretch. Experimental biology and medicine (Maywood, NJ). 2014; 239:907–912.
120. López-Sendón J, Gurfinkel EP, Lopez de Sa E, Agnelli G, Gore JM, Steg PG, Eagle KA, Cantador JR, Fitzgerald G, Granger CB, Investigators ftGRoACE. Factors related to heart rupture in acute coronary syndromes in the Global Registry of Acute Coronary Events. European heart journal. 2010; 31:1449–1456. [PubMed: 20231153]
121. López B, González A, Hermida N, Valencia F, de Teresa E, Díez J. Role of lysyl oxidase in myocardial fibrosis: from basic science to clinical aspects. American Journal of Physiology - Heart and Circulatory Physiology. 2010; 299:H1–H9. [PubMed: 20472764]
122. Louch WE, Sheehan KA, Wolska BM. Methods in cardiomyocyte isolation, culture, and gene transfer. Journal of molecular and cellular cardiology. 2011; 51:288–298. [PubMed: 21723873]
123. Lund LH, Matthews J, Aaronson K. Patient selection for left ventricular assist devices. Eur J Heart Fail. 2010; 12:434–443. [PubMed: 20172939]
124. Ma Y, Halade GV, Zhang J, Ramirez TA, Levin D, Voorhees AP, Jin YF, Han HC, Manicone AM, Lindsey M. Matrix Metalloproteinase-28 Deletion Exacerbates Cardiac Dysfunction and Rupture Following Myocardial Infarction in Mice by Inhibiting M2 Macrophage Activation. Circ Res. 2012; 20:20.

125. Majkut S, Dingal PC, Discher DE. Stress sensitivity and mechanotransduction during heart development. Curr Biol. 2014; 24:R495–501. [PubMed: 24845682]

126. Makino, A.; Prossnitz, ER.; Bünemann, M.; Wang, JM.; Yao, W.; Schmid-Schönbein, GW. G protein-coupled receptors serve as mechanosensors for fluid shear stress in neutrophils. 2006.

127. Makino A, Shin HY, Komai Y, Fukuda S, Coughlin M, Sugihara-Seki M, Schmid-Schonbein GW. Mechanotransduction in leukocyte activation: a review. Biorheology. 2007; 44:221–249. [PubMed: 18094448]

128. Malhotra R, Sadoshima J, Brosius FC 3rd, Izumo S. Mechanical stretch and angiotensin II differentially upregulate the renin-angiotensin system in cardiac myocytes In vitro. Circ Res. 1999; 85:137–146. [PubMed: 10417395]

129. Marcucci C, Lauer R, Mahajan A. New Echocardiographic Techniques for Evaluating Left Ventricular Myocardial Function. Seminars in Cardiothoracic and Vascular Anesthesia. 2008; 12:228–247. [PubMed: 19033270]

130. Matsui Y, Morimoto J, Uede T. Role of matricellular proteins in cardiac tissue remodeling after myocardial infarction. World journal of biological chemistry. 2010; 1:69–80. [PubMed: 21540992]

131. Maurer MS, Kronzon I, Burkhoff D. Ventricular Pump Function in Heart Failure with Normal Ejection Fraction: Insights from Pressure-Volume Measurements. Progress in Cardiovascular Diseases. 2006; 49:182–195. [PubMed: 17084178]

132. McDonald KS. The interdependence of Ca2+ activation, sarcomere length, and power output in the heart. Pflugers Archiv : European journal of physiology. 2011; 462:61–67. [PubMed: 21404040]

133. McManus DD, Chinali M, Saczynski JS, Gore JM, Yarzebski J, Spencer FA, Lessard D, Goldberg RJ. 30-year trends in heart failure in patients hospitalized with acute myocardial infarction. Am J Cardiol. 2011; 107:353–359. [PubMed: 21256998]

134. McNally EM, Golbus JR, Puckelwartz MJ. Genetic mutations and mechanisms in dilated cardiomyopathy. J Clin Invest. 2013; 123:19–26. [PubMed: 23281406]

135. McWhorter FY, Wang T, Nguyen P, Chung T, Liu WF. Modulation of macrophage phenotype by cell shape. Proceedings of the National Academy of Sciences. 2013; 110:17253–17258.

136. Merryman, WD.; Youn, I.; Lukoff, HD.; Krueger, PM.; Guilak, F.; Hopkins, RA.; Sacks, MS. Correlation between heart valve interstitial cell stiffness and transvalvular pressure: implications for collagen biosynthesis. 2006.

137. Metra M, Bettari L, Carubelli V, Bugatti S, Dei Cas A, Del Magro F, Lazzarini V, Lombardi C, Dei Cas L. Use of Inotropic Agents in Patients with Advanced Heart Failure. Drugs. 2011; 71:515–525. [PubMed: 21443277]

138. Mirsky I. Left ventricular stresses in the intact human heart. Biophysical journal. 1969; 9:189–208. [PubMed: 5764228]

139. Mizuno T, Yau TM, Weisel RD, Kiani CG, Li RK. Elastin stabilizes an infarct and preserves ventricular function. Circulation. 2005; 112:I81–I88. [PubMed: 16159870]

140. Moore CC, McVeigh ER, Zerhouni EA. Noninvasive measurement of three-dimensional myocardial deformation with tagged magnetic resonance imaging during graded local ischemia. Journal of cardiovascular magnetic resonance : official journal of the Society for Cardiovascular Magnetic Resonance. 1999; 1:207–222. [PubMed: 11550355]

141. Mor-Avi V, Lang RM, Badano LP, Belohlavek M, Cardim NM, Derumeaux G, Galderisi M, Marwick T, Nagueh SF, Sengupta PP, Sicari R, Smiseth OA, Smulevitz B, Takeuchi M, Thomas JD, Vannan M, Voigt JU, Zamorano JL. Current and evolving echocardiographic techniques for the quantitative evaluation of cardiac mechanics: ASE/EAE consensus statement on methodology and indications endorsed by the Japanese Society of Echocardiography. Eur J Echocardiogr. 2011; 12:167–205. [PubMed: 21385887]

142. Moustakidis P, Maniar HS, Cupps BP, Absi T, Zheng J, Guccione JM, Sundt TM, Pasque MK. Altered left ventricular geometry changes the border zone temporal distribution of stress in an experimental model of left ventricular aneurysm: a finite element model study. Circulation. 2002; 106:I168–175. [PubMed: 12354728]

143. Mullins PD, Bondarenko VE. A mathematical model of the mouse ventricular myocyte contraction. Plos One. 2013; 8:e63141. [PubMed: 23671664]

144. Nagueh SF, Appleton CP, Gillebert TC, Marino PN, Oh JK, Smiseth OA, Waggoner AD, Flachskampf FA, Pellikka PA, Evangelista A. Recommendations for the evaluation of left ventricular diastolic function by echocardiography. J Am Soc Echocardiogr. 2009; 22:107–133. [PubMed: 19187853]

145. Oishi S, Sasano T, Tateishi Y, Tamura N, Isobe M, Furukawa T. Stretch of atrial myocytes stimulates recruitment of macrophages via ATP released through gap-junction channels. Journal of pharmacological sciences. 2012; 120:296–304. [PubMed: 23196902]

146. Omens JH, Fung YC. Residual strain in rat left ventricle. Circ Res. 1990; 66:37–45. [PubMed: 2295143]

147. Oshinski JN, Han HC, Ku DN, Pettigrew RI. Quantitative prediction of improvement in cardiac function after revascularization with MR imaging and modeling: initial results. Radiology. 2001; 221:515–522. [PubMed: 11687698]

148. Oya K, Sakamoto N, Sato M. Hypoxia suppresses stretch-induced elongation and orientation of macrophages. Bio-medical materials and engineering. 2013; 23:463–471. [PubMed: 24165549]

149. Ozaki Y, Imanishi T, Tanimoto T, Teraguchi I, Nishiguchi T, Orii M, Shiono Y, Shimamura K, Yamano T, Ino Y, Yamaguchi T, Kubo T, Akasaka T. Effect of direct renin inhibitor on left ventricular remodeling in patients with primary acute myocardial infarction. Int Heart J. 2014; 55:17–21. [PubMed: 24463924]

150. Patel NR, Bole M, Chen C, Hardin CC, Kho AT, Mih J, Deng L, Butler J, Tschumperlin D, Fredberg JJ, Krishnan R, Koziel H. Cell elasticity determines macrophage function. Plos One. 2012; 7:e41024. [PubMed: 23028423]

151. Patterson SW, Starling EH. On the mechanical factors which determine the output of the ventricles. The Journal of physiology. 1914; 48:357–379. [PubMed: 16993262]

152. Paulus WJ, Tschöpe C, Sanderson JE, Rusconi C, Flachskampf FA, Rademakers FE, Marino P, Smiseth OA, De Keulenaer G, Leite-Moreira AF, Borbély A, Édes I, Handoko ML, Heymans S, Pezzali N, Pieske B, Dickstein K, Fraser AG, Brutsaert DL. How to diagnose diastolic heart failure: a consensus statement on the diagnosis of heart failure with normal left ventricular ejection fraction by the Heart Failure and Echocardiography Associations of the European Society of Cardiology. European Heart Journal. 2007; 28:2539–2550. [PubMed: 17428822]

153. Pavo N, Charwat S, Nyolczas N, Jakab A, Murlasits Z, Bergler-Klein J, Nikfardjam M, Benedek I, Benedek T, Pavo IJ, Gersh BJ, Huber K, Maurer G, Gyongyosi M. Cell therapy for human ischemic heart diseases: Critical review and summary of the clinical experiences. J Mol Cell Cardiol. 2014; 75C:12–24. [PubMed: 24998410]

154. Peterson KL, Tsuji J, Johnson A, DiDonna J, LeWinter M. Diastolic left ventricular pressure-volume and stress-strain relations in patients with valvular aortic stenosis and left ventricular hypertrophy. Circulation. 1978; 58:77–89. [PubMed: 148335]

155. Petroll WM, Ma L, Jester JV. Direct correlation of collagen matrix deformation with focal adhesion dynamics in living corneal fibroblasts. J Cell Sci. 2003; 116:1481–1491. [PubMed: 12640033]

156. Pfeiffer ER, Tangney JR, Omens JH, McCulloch AD. Biomechanics of cardiac electromechanical coupling and mechanoelectric feedback. J Biomech Eng. 2014; 136:021007. [PubMed: 24337452]

157. Pinto JG, Fung YC. Mechanical properties of the heart muscle in the passive state. J Biomech. 1973; 6:597–616. [PubMed: 4757479]

158. Pinto JG, Fung YC. Mechanical properties of the stimulated papillary muscle in quick-release experiments. J Biomech. 1973; 6:617–630. [PubMed: 4757480]

159. Rabbah JP, Saikrishnan N, Siefert AW, Santhanakrishnan A, Yoganathan AP. Mechanics of healthy and functionally diseased mitral valves: a critical review. J Biomech Eng. 2013; 135:021007. [PubMed: 23445052]

160. Rassier DE, Pavlov I. Contractile characteristics of sarcomeres arranged in series or mechanically isolated from myofibrils. Adv Exp Med Biol. 2010; 682:123–140. [PubMed: 20824523]

161. Ren J, Wold LE. Measurement of Cardiac Mechanical Function in Isolated Ventricular Myocytes from Rats and Mice by Computerized Video-Based Imaging. Biol Proced Online. 2001; 3:43–53. [PubMed: 12734580]
162. Rice JJ, Wang F, Bers DM, de Tombe PP. Approximate model of cooperative activation and crossbridge cycling in cardiac muscle using ordinary differential equations. Biophysical journal. 2008; 95:2368–2390. [PubMed: 18234826]
163. Rienks M, Papageorgiou A-P, Frangogiannis NG, Heymans S. Myocardial Extracellular Matrix: An Ever-Changing and Diverse Entity. Circulation Research. 2014; 114:872–888. [PubMed: 24577967]
164. Rouillard AD, Holmes JW. Coupled agent-based and finite-element models for predicting scar structure following myocardial infarction. Prog Biophys Mol Biol. 2014
165. Rouillard AD, Holmes JW. Mechanical regulation of fibroblast migration and collagen remodeling in healing myocardial infarcts. The Journal of Physiology. 2012
166. Sacks MS, Merryman WD, Schmidt DE. On the biomechanics of heart valve function. J Biomech. 2009; 42:1804–1824. [PubMed: 19540499]
167. Sacks MS, Yoganathan AP. Heart valve function: a biomechanical perspective. Philosophical transactions of the Royal Society of London Series B, Biological sciences. 2007; 362:1369–1391. [PubMed: 17588873]
168. Sagawa K. The ventricular pressure-volume diagram revisited. Circulation Research. 1978; 43:677–687. [PubMed: 361275]
169. Sarnoff SJ, Berglund E. Ventricular Function: I. Starling's Law of the Heart Studied by Means of Simultaneous Right and Left Ventricular Function Curves in the Dog. Circulation. 1954; 9:706–718. [PubMed: 13161102]
170. Schramm W. The units of measurement of the ventricular stroke work: a review study. J Clin Monit Comput. 2010; 24:213–217. [PubMed: 20473780]
171. Segers P, Stergiopulos N, Schreuder JJ, Westerhof BE, Westerhof N. Left ventricular wall stress normalization in chronic pressure- overloaded heart: a mathematical model study. Am J Physiol Heart Circ Physiol. 2000; 279:H1120–1127. [PubMed: 10993775]
172. Senni M, Paulus WJ, Gavazzi A, Fraser AG, Díez J, Solomon SD, Smiseth OA, Guazzi M, Lam CSP, Maggioni AP, Tschöpe C, Metra M, Hummel SL, Edelmann F, Ambrosio G, Stewart Coats AJ, Filippatos GS, Gheorghiade M, Anker SD, Levy D, Pfeffer MA, Stough WG, Pieske BM. New strategies for heart failure with preserved ejection fraction: the importance of targeted therapies for heart failure phenotypes. European heart journal. 2014
173. Shadwick RE. Mechanical design in arteries. Journal of Experimental Biology. 1999; 202:3305–3313. [PubMed: 10562513]
174. Shamhart PE, Meszaros JG. Non-fibrillar collagens: Key mediators of post-infarction cardiac remodeling? Journal of molecular and cellular cardiology. 2010; 48:530–537. [PubMed: 19573533]
175. Shi F, Harman J, Fujiwara K, Sottile J. Collagen I matrix turnover is regulated by fibronectin polymerization. American Journal of Physiology - Cell Physiology. 2010; 298:C1265–C1275. [PubMed: 20107040]
176. Shimazaki M, Nakamura K, Kii I, Kashima T, Amizuka N, Li M, Saito M, Fukuda K, Nishiyama T, Kitajima S, Saga Y, Fukayama M, Sata M, Kudo A. Periostin is essential for cardiac healingafter acute myocardial infarction. J Exp Med. 2008; 205:295–303. [PubMed: 18208976]
177. Skrzypiec-Spring M, Grotthus B, Szelag A, Schulz R. Isolated heart perfusion according to Langendorff---still viable in the new millennium. J Pharmacol Toxicol Methods. 2007; 55:113–126. [PubMed: 16844390]
178. Stampehl MR, Mann DL, Nguyen JS, Cota F, Colmenares C, Dokainish H. Speckle Strain Echocardiography Predicts Outcome in Patients with Heart Failure with both Depressed and Preserved Left Ventricular Ejection Fraction. Echocardiography. 2014
179. Taber LA. Biomechanics of cardiovascular development. Annual review of biomedical engineering. 2001; 3:1–25.
180. Taber LA. Biophysical mechanisms of cardiac looping. Int J Dev Biol. 2006; 50:323–332. [PubMed: 16479500]

181. Taber LA, Chabert S. Theoretical and experimental study of growth and remodeling in the developing heart. Biomechanics and modeling in mechanobiology. 2002; 1:29–43. [PubMed: 14586705]

182. Taber LA, Voronov DA, Ramasubramanian A. The role of mechanical forces in the torsional component of cardiac looping. Ann N Y Acad Sci. 2010; 1188:103–110. [PubMed: 20201892]

183. Takeuchi M, Nakai H, Kokumai M, Nishikage T, Otani S, Lang RM. Age-related changes in left ventricular twist assessed by two-dimensional speckle-tracking imaging. J Am Soc Echocardiogr. 2006; 19:1077–1084. [PubMed: 16950461]

184. Tetsunaga T, Nishida K, Furumatsu T, Naruse K, Hirohata S, Yoshida A, Saito T, Ozaki T. Regulation of mechanical stress-induced MMP-13 and ADAMTS-5 expression by RUNX-2 transcriptional factor in SW1353 chondrocyte-like cells. Osteoarthritis and Cartilage. 2011; 19:222–232. [PubMed: 21094261]

185. Thavendiranathan P, Poulin F, Lim KD, Plana JC, Woo A, Marwick TH. Use of myocardial strain imaging by echocardiography for the early detection of cardiotoxicity in patients during and after cancer chemotherapy: a systematic review. J Am Coll Cardiol. 2014; 63:2751–2768. [PubMed: 24703918]

186. Thebault C, Donal E, Bernard A, Moreau O, Schnell F, Mabo P, Leclercq C. Real-time three-dimensional speckle tracking echocardiography: a novel technique to quantify global left ventricular mechanical dyssynchrony. European Journal of Echocardiography. 2011; 12:26–32. [PubMed: 20736292]

187. Thomas KL, Velazquez EJ. Therapies to prevent heart failure post-myocardial infarction. Curr Heart Fail Rep. 2005; 2:174–182. [PubMed: 16332310]

188. Tobita K, Garrison JB, Liu LJ, Tinney JP, Keller BB. Three-dimensional myofiber architecture of the embryonic left ventricle during normal development and altered mechanical loads. The anatomical record Part A, Discoveries in molecular, cellular, and evolutionary biology. 2005; 283:193–201.

189. Trayanova NA, Rice JJ. Cardiac Electromechanical Models: From Cell to Organ. Frontiers in Physiology. 2011:2. [PubMed: 21423412]

190. Tromp J, van der Pol A, Klip IT, de Boer RA, Jaarsma T, van Gilst WH, Voors AA, van Veldhuisen DJ, van der Meer P. Fibrosis Marker Syndecan-1 and Outcome in Patients With Heart Failure With Reduced and Preserved Ejection Fraction. Circulation: Heart Failure. 2014; 7:457–462. [PubMed: 24647119]

191. Vieira MJ, Teixeira R, Goncalves L, Gersh BJ. Left atrial mechanics: echocardiographic assessment and clinical implications. J Am Soc Echocardiogr. 2014; 27:463–478. [PubMed: 24656882]

192. Villarreal FJ, Dillmann WH. Cardiac hypertrophy-induced changes in mRNA levels for TGF-beta 1, fibronectin, and collagen. Am J Physiol. 1992; 262:H1861–1866. [PubMed: 1535758]

193. Voelkel NF, Quaife RA, Leinwand LA, Barst RJ, McGoon MD, Meldrum DR, Dupuis J, Long CS, Rubin LJ, Smart FW, Suzuki YJ, Gladwin M, Denholm EM, Gail DB. Right Ventricular Function and Failure: Report of a National Heart, Lung, and Blood Institute Working Group on Cellular and Molecular Mechanisms of Right Heart Failure. Circulation. 2006; 114:1883–1891. [PubMed: 17060398]

194. Voorhees, A.; DeLeon, KY.; Ma, Y.; Halade, GV.; Yabluchanskiy, A.; Lindsey, ML.; Han, HC. Cardiac Mechanics in Matrix Metalloproteinase-9 Null Mice Post-Myocardial Infarction; BMES Annual Meeting; Seattle, WA. 2013;

195. Voorhees A, Han H-C. A model to determine the effect of collagen fiber alignment on heart function post myocardial infarction. Theoretical Biology and Medical Modelling. 2014; 11:6. [PubMed: 24456675]

196. Wagenseil, JE.; Mecham, RP. Vascular Extracellular Matrix and Arterial Mechanics. 2009.

197. Waldman LK, Nosan D, Villarreal F, Covell JW. Relation between transmural deformation and local myofiber direction in canine left ventricle. Circ Res. 1988; 63:550–562. [PubMed: 3409487]

198. Walker JC, Ratcliffe MB, Zhang P, Wallace AW, Hsu EW, Saloner DA, Guccione JM. Magnetic resonance imaging-based finite element stress analysis after linear repair of left ventricular aneurysm. J Thorac Cardiovasc Surg. 2008; 135:1094–U1057. [PubMed: 18455590]

199. Wall ST, Guccione JM, Ratcliffe MB, Sundnes JS. Electromechanical feedback with reduced cellular connectivity alters electrical activity in an infarct injured left ventricle: a finite element model study. Am J Physiol Heart Circ Physiol. 2012; 302:H206–214. [PubMed: 22058157]

200. Wang B, Wang G, To F, Butler JR, Claude A, McLaughlin RM, Williams LN, de Jongh Curry AL, Liao J. Myocardial scaffold-based cardiac tissue engineering: application of coordinated mechanical and electrical stimulations. Langmuir. 2013; 29:11109–11117. [PubMed: 23923967]

201. Wang BW, Hung HF, Chang H, Kuan P, Shyu KG. Mechanical stretch enhances the expression of resistin gene in cultured cardiomyocytes via tumor necrosis factor-alpha. Am J Physiol Heart Circ Physiol. 2007; 293:H2305–2312. [PubMed: 17573461]

202. Wang HM, Gao H, Luo XY, Berry C, Griffith BE, Ogden RW, Wang TJ. Structure-based finite strain modelling of the human left ventricle in diastole. International journal for numerical methods in biomedical engineering. 2013; 29:83–103. [PubMed: 23293070]

203. Wang HM, Luo XY, Gao H, Ogden RW, Griffith BE, Berry C, Wang TJ. A modified Holzapfel-Ogden law for a residually stressed finite strain model of the human left ventricle in diastole. Biomechanics and modeling in mechanobiology. 2014; 13:99–113. [PubMed: 23609894]

204. Warwick R, Pullan M, Poullis M. Mathematical modelling to identify patients who should not undergo left ventricle remodelling surgery. Interactive CardioVascular and Thoracic Surgery. 2010; 10:661–665. [PubMed: 20093268]

205. Weber KT, Sun Y, Tyagi SC, Cleutjens JP. Collagen network of the myocardium: function, structural remodeling and regulatory mechanisms. J Mol Cell Cardiol. 1994; 26:279–292. [PubMed: 8028011]

206. Weis SM, Zimmerman SD, Shah M, Covell JW, Omens JH, Ross J Jr, Dalton N, Jones Y, Reed CC, Iozzo RV, McCulloch AD. A role for decorin in the remodeling of myocardial infarction. Matrix Biology. 2005; 24:313–324. [PubMed: 15949932]

207. Wenk JF, Eslami P, Zhang Z, Xu C, Kuhl E, Gorman JH Iii, Robb JD, Ratcliffe MB, Gorman RC, Guccione JM. A Novel Method for Quantifying the In-Vivo Mechanical Effect of Material Injected Into a Myocardial Infarction. The Annals of Thoracic Surgery. 2011; 92:935–941. [PubMed: 21871280]

208. Wildgruber M, Bielicki I, Aichler M, Kosanke K, Feuchtinger A, Settles M, Onthank DC, Cesati RR, Robinson SP, Huber AM, Rummeny EJ, Walch AK, Botnar RM. Assessment of myocardial infarction and postinfarction scar remodeling with an elastin-specific magnetic resonance agent. Circ Cardiovasc Imaging. 2014; 7:321–329. [PubMed: 24363356]

209. Windecker S, Kolh P, Alfonso F, Collet JP, Cremer J, Falk V, Filippatos G, Hamm C, Head SJ, Juni P, Kappetein AP, Kastrati A, Knuuti J, Landmesser U, Laufer G, Neumann FJ, Richter DJ, Schauerte P, Sousa Uva M, Stefanini GG, Taggart DP, Torracca L, Valgimigli M, Wijns W, Witkowski A. 2014 ESC/EACTS Guidelines on myocardial revascularization: The Task Force on Myocardial Revascularization of the European Society of Cardiology (ESC) and the European Association for Cardio-Thoracic Surgery (EACTS) Developed with the special contribution of the European Association of Percutaneous Cardiovascular Interventions (EAPCI). EuroIntervention : journal of EuroPCR in collaboration with the Working Group on Interventional Cardiology of the European Society of Cardiology. 2014

210. Wood P, Piran S, Liu PP. Diastolic Heart Failure: Progress, Treatment Challenges, and Prevention. Canadian Journal of Cardiology. 2011; 27:302–310. [PubMed: 21601770]

211. Yabluchanskiy A, Ma Y, Chiao YA, Lopez EF, Voorhees AP, Toba H, Hall ME, Han H-C, Lindsey ML, Jin Y-F. Cardiac aging is initiated by matrix metalloproteinase-9 mediated endothelial dysfunction. American Journal of Physiology - Heart and Circulatory Physiology. 2014

212. Yabluchanskiy A, Ma Y, Deleon-Pennell K, Jin Y-F, Lindsey M. Matrix metalloproteinase-9 deletion shifts macrophage polarization towards M2 phenotype in aged left ventricles post-myocardial infarction. Cardiovascular Research. 2014; 103:S6.

213. Yamakawa M, Kyo S, Yamakawa S, Ono M, Kinugawa K, Nishimura T. Destination therapy: the new gold standard treatment for heart failure patients with left ventricular assist devices. Gen Thorac Cardiovasc Surg. 2013; 61:111–117. [PubMed: 23264080]

214. Yamashita O, Yoshimura K, Nagasawa A, Ueda K, Morikage N, Ikeda Y, Hamano K. Periostin links mechanical strain to inflammation in abdominal aortic aneurysm. Plos One. 2013; 8:e79753. [PubMed: 24260297]

215. Yambe M, Tomiyama H, Hirayama Y, Gulniza Z, Takata Y, Koji Y, Motobe K, Yamashina A. Arterial stiffening as a possible risk factor for both atherosclerosis and diastolic heart failure. Hypertens Res. 2004; 27:625–631. [PubMed: 15750255]

216. Yancy CW, Jessup M, Bozkurt B, Butler J, Casey DE Jr. Drazner MH, Fonarow GC, Geraci SA, Horwich T, Januzzi JL, Johnson MR, Kasper EK, Levy WC, Masoudi FA, McBride PE, McMurray JJ, Mitchell JE, Peterson PN, Riegel B, Sam F, Stevenson LW, Tang WH, Tsai EJ, Wilkoff BL, American College of Cardiology F; American Heart Association Task Force on Practice G. 2013 ACCF/AHA guideline for the management of heart failure: a report of the American College of Cardiology Foundation/American Heart Association Task Force on Practice Guidelines. Journal of the American College of Cardiology. 2013; 62:e147–239. [PubMed: 23747642]

217. Yang T, Chiao YA, Wang Y, Voorhees A, Han HC, Lindsey ML, Jin YF. Mathematical modeling of left ventricular dimensional changes in mice during aging. BMC Syst Biol. 2012; 6:1752–0509.

218. Yarbrough WM, Mukherjee R, Ikonomidis JS, Zile MR, Spinale FG. Myocardial remodeling with aortic stenosis and after aortic valve replacement: mechanisms and future prognostic implications. J Thorac Cardiovasc Surg. 2012; 143:656–664. [PubMed: 21762938]

219. Yin Z, Ren J, Guo W. Sarcomeric protein isoform transitions in cardiac muscle: A journey to heart failure. Biochimica et Biophysica Acta (BBA) - Molecular Basis of Disease. 2015; 1852:47–52. [PubMed: 25446994]

220. Yu Q, Vazquez R, Zabadi S, Watson RR, Larson DF. T-lymphocytes mediate left ventricular fibrillar collagen cross-linking and diastolic dysfunction in mice. Matrix Biol. 2010; 29:511–518. [PubMed: 20600894]

221. Zamilpa R, Lindsey ML. Extracellular matrix turnover and signaling during cardiac remodeling following MI: Causes and consequences. Journal of Molecular and Cellular Cardiology. 2010; 48:558–563. [PubMed: 19559709]

222. Zhang Y, Lin Z, Foolen J, Schoen I, Santoro A, Zenobi-Wong M, Vogel V. Disentangling the multifactorial contributions of fibronectin, collagen and cyclic strain on MMP expression and extracellular matrix remodeling by fibroblasts. Matrix Biology. 2014

223. Zhang Z, Tendulkar A, Sun K, Saloner DA, Wallace AW, Ge L, Guccione JM, Ratcliffe MB. Comparison of the Young-Laplace Law and Finite Element Based Calculation of Ventricular Wall Stress: Implications for Postinfarct and Surgical Ventricular Remodeling. The Annals of Thoracic Surgery. 2011; 91:150–156. [PubMed: 21172505]

224. Zhong J, Liu W, Yu X. Characterization of three-dimensional myocardial deformation in the mouse heart: An MR tagging study. Journal of Magnetic Resonance Imaging. 2008; 27:1263–1270. [PubMed: 18504746]

225. Zile MR, Baicu CF. Biomarkers of diastolic dysfunction and myocardial fibrosis: application to heart failure with a preserved ejection fraction. J Cardiovasc Transl Res. 2013; 6:501–515. [PubMed: 23716130]

226. Zile MR, Cowles MK, Buckley JM, Richardson K, Cowles BA, Baicu CF, Cooper GI, Gharpuray V. Gel stretch method: a new method to measure constitutive properties of cardiac muscle cells. Am J Physiol. 1998; 274:H2188–2202. [PubMed: 9841544]

227. Zile MR, Richardson K, Cowles MK, Buckley JM, Koide M, Cowles BA, Gharpuray V, Cooper Gt. Constitutive properties of adult mammalian cardiac muscle cells. Circulation. 1998; 98:567–579. [PubMed: 9714115]

228. Zimmer HG. The Isolated Perfused Heart and Its Pioneers. News Physiol Sci. 1998; 13:203–210. [PubMed: 11390791]

Further Reading

229. Humphrey, JD. Cardiovascular Solid Mechanics: Cells, Tissues, and Organs. Springer; New York: 2002.

230. Fung, YC. Biomechanics: Circulation. 2nd Ed.. Springer; New York: 1997.

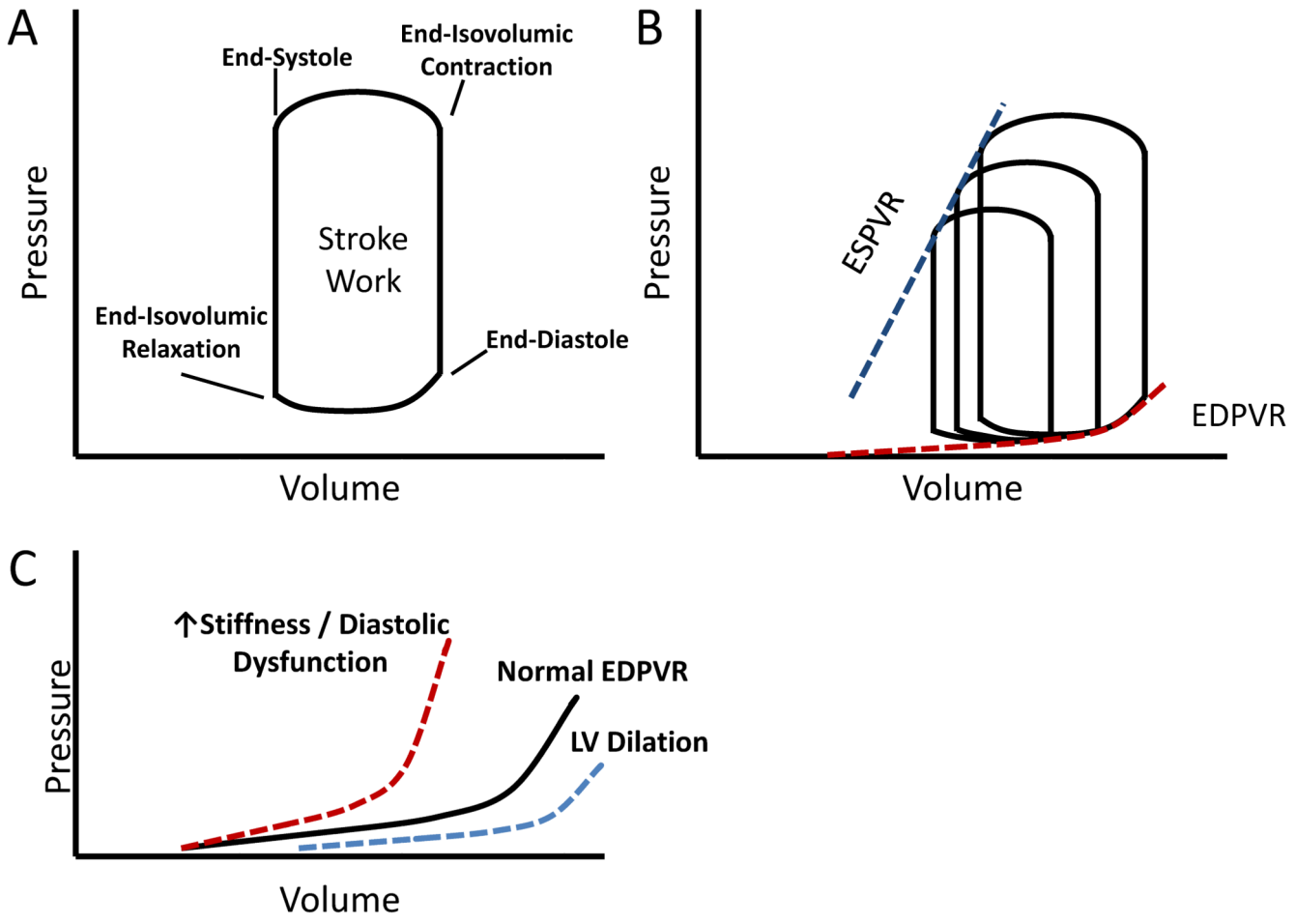

Figure 1. The Pressure Volume Relationship

A graphical representation of the pressure volume loop depicting the events of the cardiac cycle, and depicting stroke work as the area inside the loop. B. Occlusion of the vena cava reduces LV filling and allows for the determination of the end-diastolic pressure volume relationship (EDPVR) and the end-systolic pressure volume relationship (ESPVR). C. Increased myocardial stiffness leads to a leftward and upward shift of the EDPVR, reducing diastolic filling (red dotted line). Dilation of the LV can be noted as a rightward shift of the EDPVR (blue dotted line).

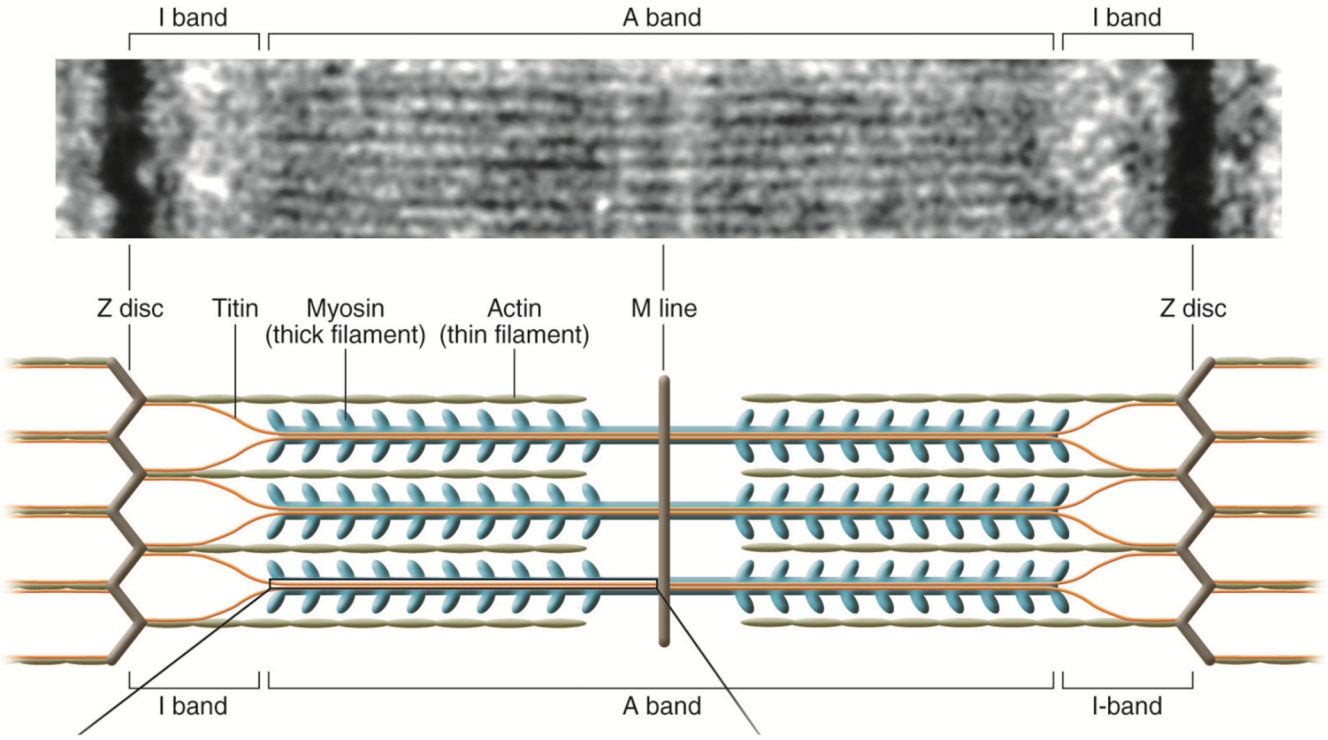

Figure 2. The Sarcomere of the Cardiac Myocyte

Titin is an elastic protein that runs from the Z band all the way to the M-line, and provides the sarcomere with its passive strength. Myosin is the motor protein of the sarcomere and its interaction with the actin filament drives cardiomyocyte contraction. Figure adapted from McNally, 2012 with permission of the American Society for Clinical Investigation (134).

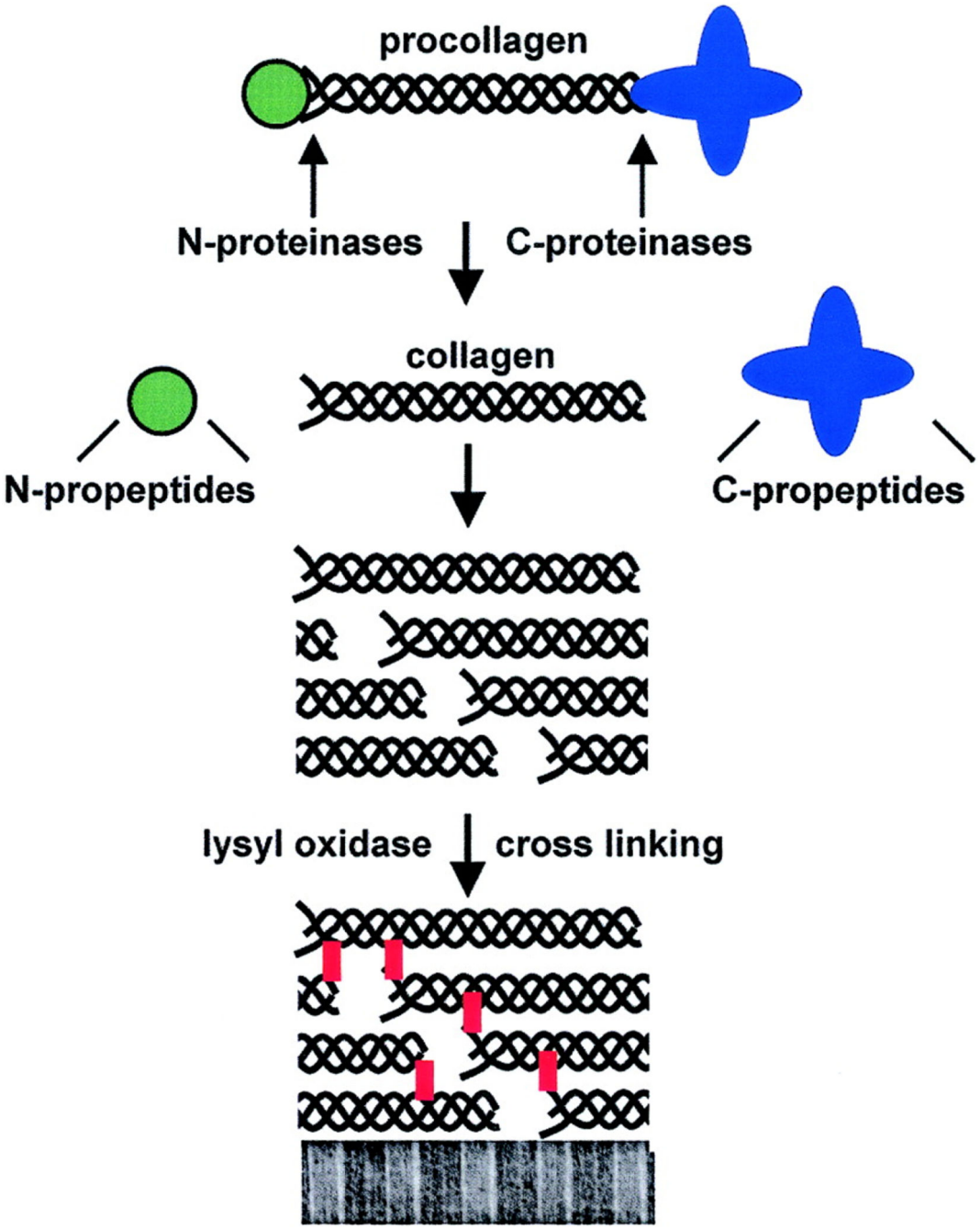

Figure 3. Collagen Fiber Structure and Assembly

Procollagen assembles as a triple helix and then has the N and C terminal ends cleaved by proteases. The collagen triple helixes then assemble into larger fibers aided by collagen cross-linking facilitated by lysyl oxidase. Figure adapted from Kadler, 2004 with permission of Elsevier (91).

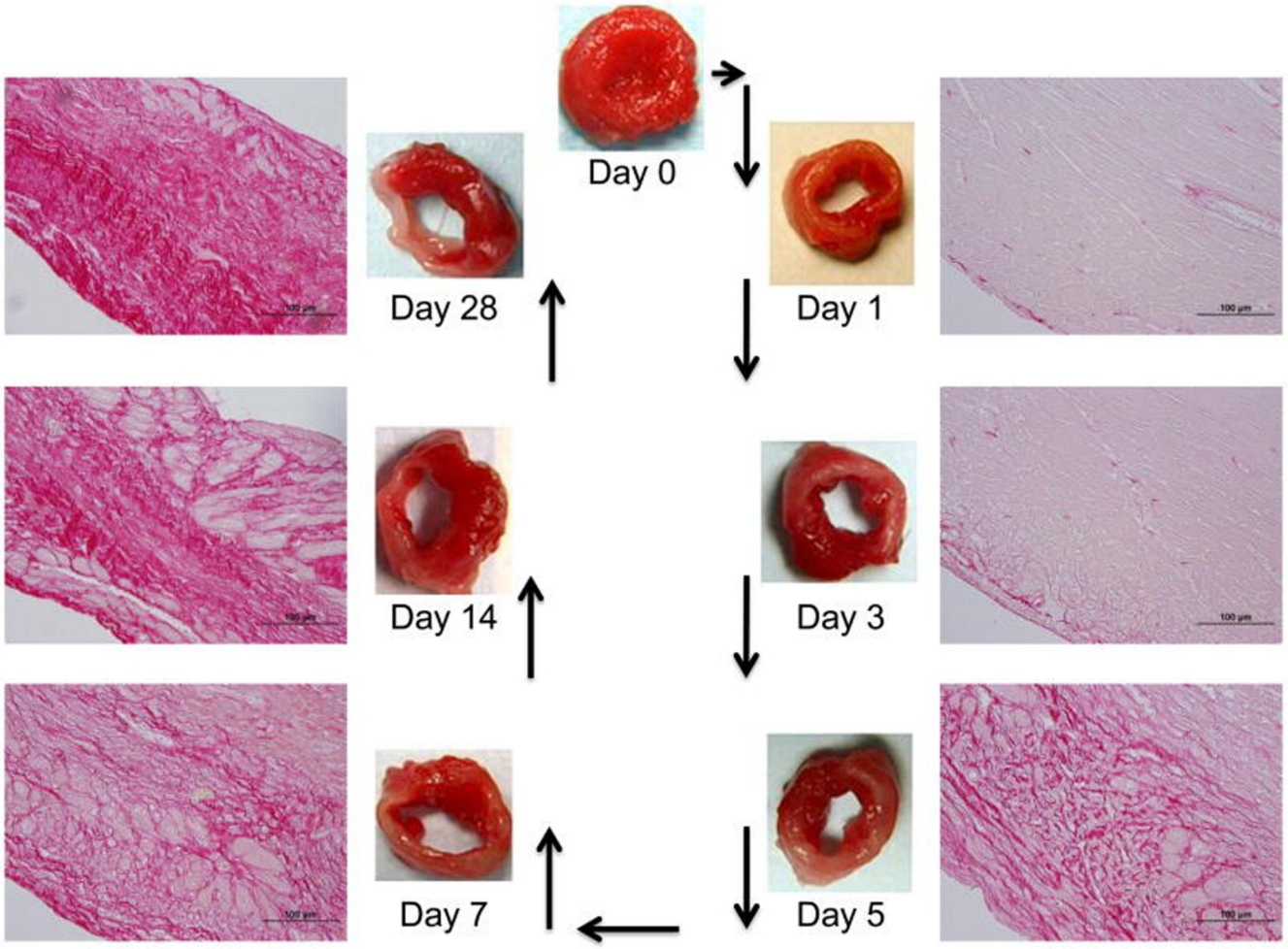

Figure 4. Progression of Left Ventricle Dilation and Remodeling Post-MI

The inner pictures display the cross-section of a mouse left ventricle stained with 1% 2,3,5-triphenyltetrazolium chloride after myocardial infarction. Significant cavity dilation and wall thinning can be observed. The outer pictures show histological sections stained with picrosirius red for collagen. An increase in collagen is seen around day 7 and by day 28 collagen fibers have become densely packed and highly aligned. Figure adapted from Zamilpa and Lindsey, 2010 with permission of Elsevier (221)

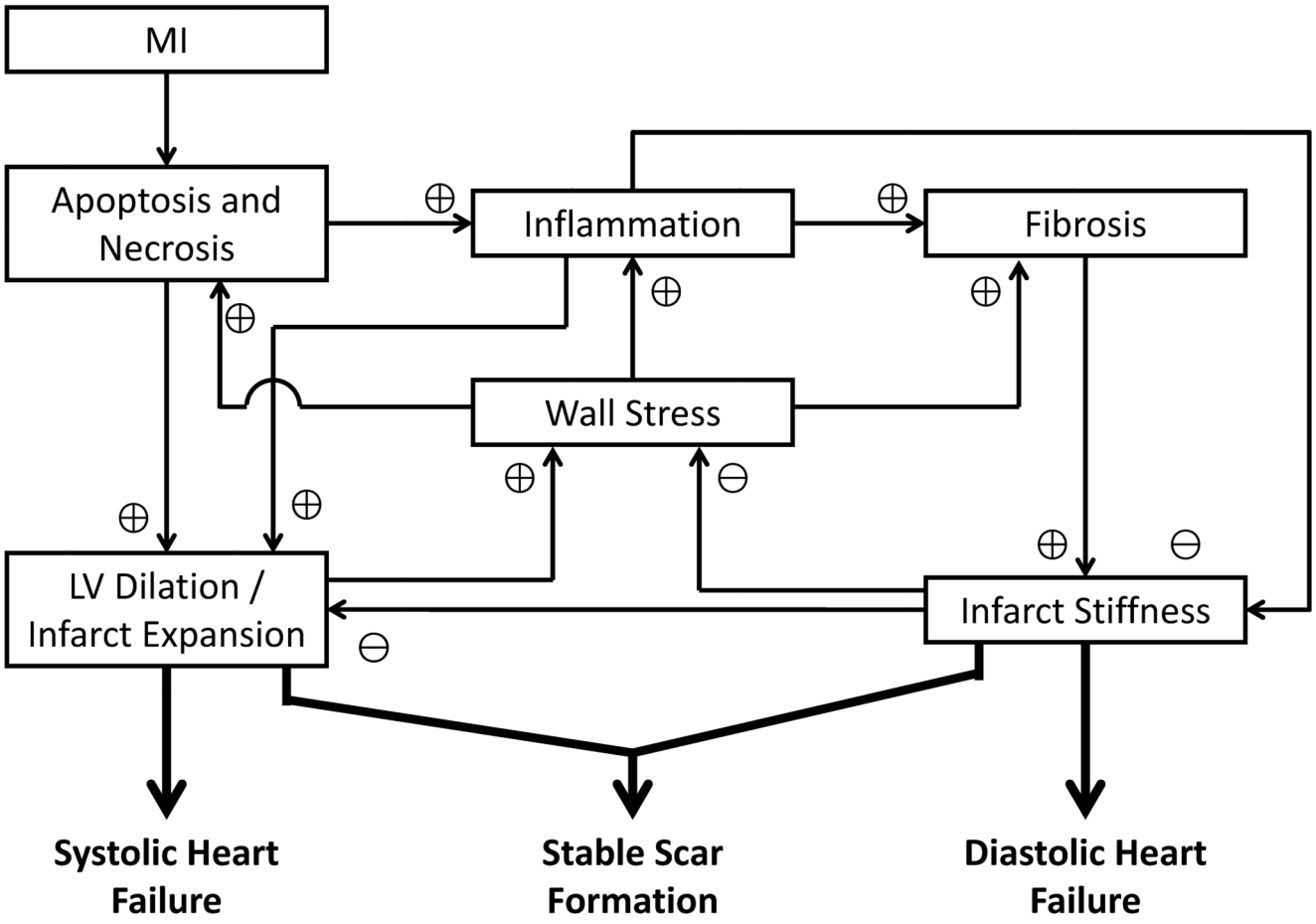

Figure 5. Regulation of MI Outcome by Mechanical Feedback

Dilation of the LV due to the loss of cellular structure increases the wall stress which in turn signals for increased inflammation and fibrosis. Inflammation reduces tissue stiffness while fibrosis increases tissue stiffness. Increased tissue stiffness in turn reduces LV stretch and dilation. Unbalances in the feedback system can lead either to systolic heart failure due to infarct expansion and LV dilation, or diastolic heart failure due to over-stiffening of the infarct. The + symbol in the schematic represents a positive correlation between the factors, i.e. increased LV dilation increases wall stresses, while the – symbol denotes a negative correlation.

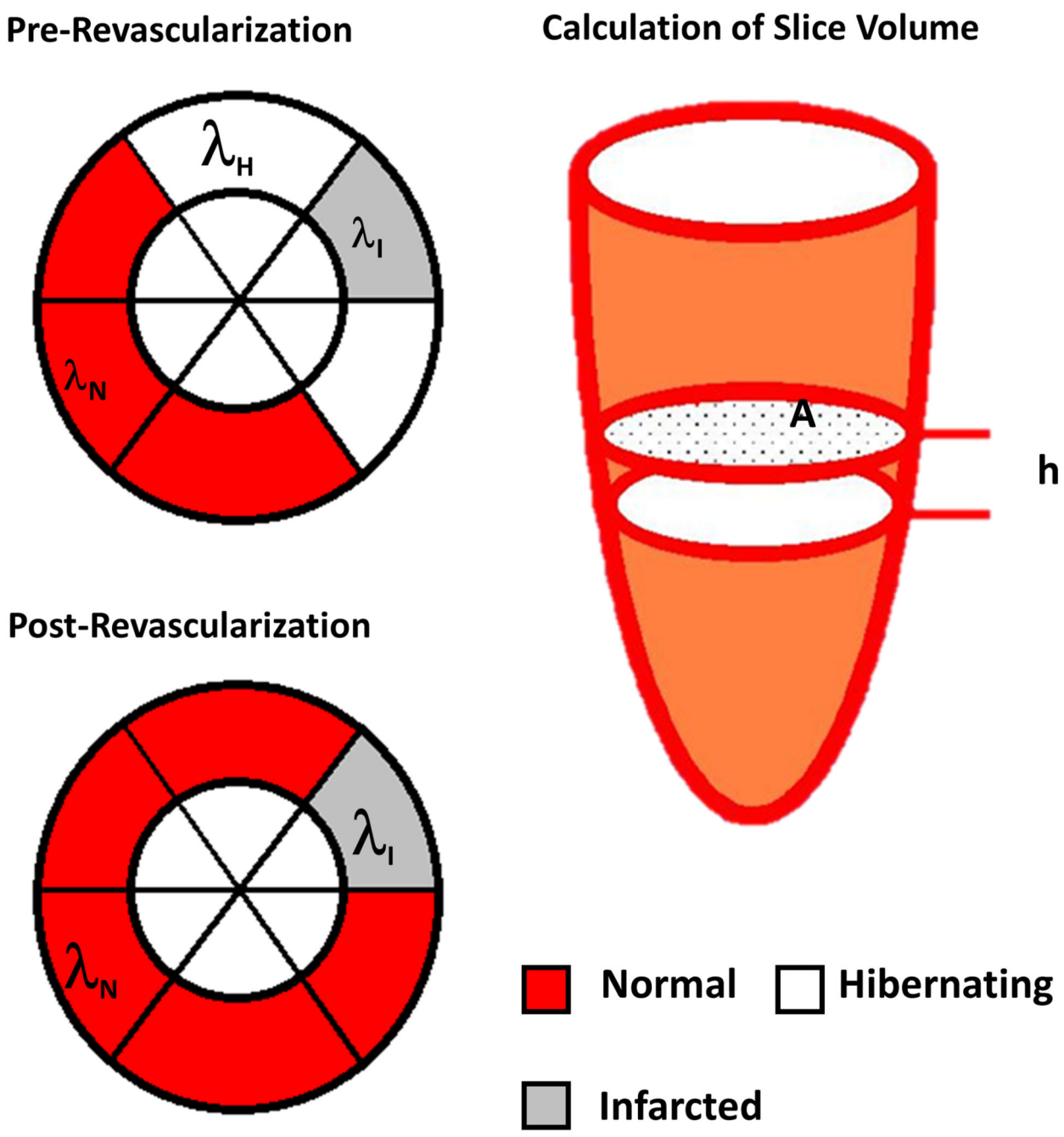

Figure 6. Myocardial viability and LV function

Schematic illustration of myocardial viability change post-revascularization and a scheme to determine the left ventricular volume from short axis slices. λ with subscript N, H, I, represent the contraction ratio in the normal, hibernating and infarct regions, respectively. The ventricular volume is determined by summation of the area (A) multiplied by slice thickness h.

Table 1
Mechanical Factors that Affect Cardiac Output

Category	Factors
Preload	venous return, diastolic wall stiffness, filling time, atrial stiffness
Contractility	sarcomere length, inotropic state
Afterload	arterial pressure, arterial resistance, aortic valve function
Heart Rate	activity level

Table 2

Measures of Cardiac Function

Measure	Description
Stroke Volume (SV)	Volume of blood pumped per beat
Ejection Fraction (EF)	Stroke volume normalized by diastolic volume
Cardiac Output (CO)	Volume of blood pumped per unit time
Stroke Work (SW)	Energy imparted to the blood by the myocardium during one beat
Global Longitudinal Strain (GLS)	Measure of longitudinal contractile ability
Global Radial Strain (GRS)	Measure of radial contractile ability
Ratio of mitral inflow velocity to early diastolic annular velocity (E/e')	Measure of diastolic function, correlated with diastolic filling pressure
dP/dt	The rate of pressure increase during systolic contraction
Time constant of ventricular relaxation (τ)	Measure of the rate of ventricular contraction

Table 3

Methods for Measuring Cardiac Function

Measurement	Methods
Dimensions and Geometry	Echocardiography, MRI, CT, SPECT, PET, MUGA
Contractile Function and Strain	Tagged MRI, Tissue Doppler Echocardiography, Speckle-Tracking Echocardiography
Pressure-Volume Relationship	Cardiac Catheterization

Table 4
Main Factors Influencing Patient Outcome Post-MI

Factor in Patient Outcome
Infarct Size
Infarct Thickness (Transmural or Non-Transmural)
Infarct Location
ST Segment Elevation
Reperfussion
Pharmaceutical Treatment
Inflammation Levels
Level of LV Remodeling
Scar Stiffness
LV Wall Stress
Age
Sex
Previous Cardiovascular Disease
Obesity
Diabetes
Hypertension
Hyperlipidaemia
Smoking Status